Norwegian University
of Life Sciences

Master's Thesis 2023 60 ECTS
Faculty of Chemistry, Biotechnology, and Food Science

Impact of nutrients on sediment microorganism composition and cobalamin activity in a marine microcosm pollution experiment

Luis Yndy Ariem Ramirez
MSc Biotechnology

Impact of nutrients on sediment microorganism composition and cobalamin activity in a marine microcosm pollution experiment

Norwegian University of Life Sciences (NMBU),

Faculty of Chemistry, Biotechnology and Food Science

Acknowledgements

The work presented for this master's thesis was conducted with the MiDiv research group at the Faculty of Chemistry, Biotechnology, and Food Science (KBM) under the supervision of Professor Knut Rudi and engineer Inga Leena Angell.

The outstanding learning environment provided by the MiDiv research group was central to the completion of this master's thesis. It has truly been a group in which academic excellence can be achieved. I gained vital theoretical knowledge and practical experience within biotechnology in a short period of time with MiDiv, and I shall be grateful for everything for as long as I live.

I want to express my gratitude to my main supervisor, Professor Knut Rudi for all the guidance and knowledge he has provided me with, and for continuing to do so even in his summer holiday. I also want to thank my secondary supervisor, Inga Leena Angell, for walking me through the practical part of the thesis and for being patient with me for the seemingly never-ending questions I have asked her for the past several months and for generating the Phyloseq plots for me. A special thanks to the remaining members/former members of the MiDiv group for all the help and insight when I was struggling in the laboratory. I am deeply grateful to you Oda Larsen Hammarheim, Tonje Nilsen, Karen Utheim, Melcy Philip, Ewelina Blanka Grad, Morten Nilsen, Ida Ormaasen, Karoline Stubmo, and Julie Martin. You all have inspired me to complete this task and have made this master's thesis far better than what I would have had without you.

Without the never-ending support of my family, this master's thesis would not have been completed in a literal sense. I have expressed my fears, worries, and doubts during the hard times of both academic and personal struggle to all of you, but your encouraging words, understanding, and unconditional love has made me realize that everything should be possible. This work is dedicated to each and every one of you. I also want to thank my friend and brother, Mats Rune Pettersen for being there in times of adversity, for playing chess with me as a therapeutic activity during those times, and for all the whimsical conversations and ideas we have shared in the Biotechnology building.

Oslo, August 2023

Luis Yndy Ariem Ramirez

Abstract

Microorganisms play crucial roles in sustaining life in the marine ecosystem including but not limited to organic matter remineralization, carbon sequestration, and nutrient production and recycling. However, the rapid growth of marine aquaculture in the past few decades may have consequences in microbiological life, especially the sediment-associated microorganisms. There have been many reports of anthropogenic sources of organic matter such as undigested food pellets and feces from fish farms affecting the composition of microbial communities within the sediments due to the development of a hypoxic/anoxic environment and overall habitat modifications.

The present study examined this by performing experimental assays based on both key observations and hypotheses by Pettersen et al. (2022). They observed that high Operational Taxonomic Unit (OTUs) was strongly associated with ammonium-oxidation reactions, and low OTU richness with denitrification. It was also observed that the ammonium-oxidizing archaeon, *Nitrosopumilus*, was associated with high OTU richness. Based on this knowledge, and that *Nitrosopumulus* is a cobalamin-implicated genus, it was also predicted that there might be a potential association between high cobalamin abundance and high OTU richness. To study these, the following media were created for a microcosm pollution experiment: ammonium-oxidizing, nitrate-reducing, and sulfate-reducing, each set at oxic and anoxic conditions. Samples from each medium were retrieved over the course of four weeks. Optimization and utilization of Enzyme-linked immunosorbent assay (ELISA) and microbiological assay were performed to determine cobalamin. 16S rRNA sequencing was then performed to gain insight on the microbial compositions within all samples from the microcosm pollution experiment.

The results of the present study showed that there was little to no detection of ammonium-oxidizing archaea within all media based on the qPCR data. High OTU richness was observed in the ammonium-oxidizing media, and low OTU richness in both nitrate- and sulfate-reducing media. Moreover, the nitrate- and sulfate-reducing media had the highest concentrations of cobalamin, while the ammonium-oxidizing media had the lowest, which might be linked to the growth of a cobalamin-implicated genus, *Propionigenium*, in both nitrate- and sulfate-reducing media. Further research to verify the correlation between cobalamin abundance and OTU richness must be done. In addition, the role of *Propionigenium* in cobalamin production within the marine benthic ecosystem must be included in future investigations.

Sammendrag

Mikroorganismer spiller avgjørende roller for å opprettholde liv i det marine økosystemet, som remineralisering av organisk materiale, karbonbinding, og resirkulering og produksjon av næringsstoffer. Imidlertid kan den raske veksten av marin akvakultur de siste tiårene ha konsekvenser for det mikrobiologiske livet, spesielt for de sedimentassosierte mikroorganismene. Det har vært mange studier om antropogene kilder til organisk materiale forurensning som ufordøyd matpellets og avføring fra oppdrettsanlegg som påvirker sammensetningen av det mikrobielle samfunnet i sedimentene på grunn av utviklingen av et hypoksisk/anoksisk miljø og generelle habitatmodifikasjoner.

Denne studien undersøkte dette ved å utføre eksperimentelle analyser basert på både sentrale observasjoner og hypoteser av Pettersen et al. (2022). De observerte at høy Operational Taxonomic Units (OTUs) var sterkt assosiert med ammoniumoksidasjonsreaksjoner, og lavt OTU diversitet med denitrifikasjon. Det ble også observert at den ammoniumoksiderende arkeonen, *Nitrosopumilus*, var assosiert med høyt OTU diversitet. Basert på denne observasjonen og det at *Nitrosopumilus* er et kobalamin-implisert slekt, ble det forutsatt at det kan være en potensiell sammenheng mellom høy kobalamin mengde og høy OTU diversitet. For å studere disse ble følgende medier laget for et anrikningseksperiment: ammoniumoksiderende, nitratreduserende og sulfatreduserende, satt til oksiske og anoksiske forhold. Prøver fra hvert medium ble hentet i løpet av fire uker. Optimalisering og bruk av Enzyme-linked immunosorbent assay (ELISA) og mikrobiologisk analyse ble utført for å måle kobalamin. 16S rRNA-sekvensering ble også utført for å få kunnskap om den mikrobielle sammensetningen i hver prøve fra anrikningen.

Resultatene av denne studien viste at det var liten eller ingen påvisning av ammoniumoksiderende arkea i alle medier basert på qPCR-dataene. Høy OTU diversitet ble observert i ammoniumoksiderende medier, og lav OTU diversitet i både nitrat- og sulfatreduserende medier. Dessuten hadde de nitrat- og sulfatreduserende media de høyeste kobalaminkonsentrasjonene, mens de ammoniumoksiderende media hadde de laveste, noe som kan være knyttet til veksten av et kobalamin-implisert slekt, *Propionigenium*, i både nitrat- og sulfatreduserende medier. Ytterligere forskning for å bekrefte sammenhengen mellom kobalaminmengde og OTU diversitet må gjøres. I tillegg må *Propionigeniums* rolle i kobalaminproduksjonen i det marine bentiske økosystemet inkluderes i fremtidige undersøkelser.

Abbreviations

AdoCbl – Adenosylcobalamin

AmoA – ammonium-oxidizing archaea

AO(A) – Ammonium-oxidizing (Anoxic)

AO(O) – Ammonium-oxidizing (Oxic)

ATCC – American Type Culture Collection

CobS – Cobalamin Synthase

C_q – Quantification cycles

ddNTP - Dideoxynucleotide triphosphates

DMB – Dimethylbenzimidizole

DNA – Deoxyribonucleic acid

dNTPs – Deoxynucleotide triphosphates

DW – Deep well

EDTA – Ethylenediaminetetraacetic Acid

ELISA – Enzyme-linked immunosorbent assay

EPS – Extracellular Polymeric Substances

GDP – Gross Domestic Product

HPLC – High-performance Liquid Chromatography

MeCbl – Methylcobalamin

NGS – Next Generation Sequencing

NR(A) – Nitrate-reducing (Anoxic)

NR(O) – Nitrate-reducing (Oxic)

OD – Optical Density

OTU – Operational Taxonomic Unit

PBS – Phosphate Buffered Saline

PcoA – Principal coordinates analysis

PCR – Polymerase Chain Reaction

qPCR – Quantitative Polymerase Chain Reaction

RIA – Radioimmunoassay

RNA – Ribonucleic acid

rRNA – Ribosomal ribonucleic acid

SBS – Sequencing by Synthesis

SNP - Single nucleotide polymorphism

SR(A) – Sulfate-reducing (Anoxic)

SR(O) – Sulfate-reducing (Oxic)

STAR – Stool Transport and Recover

TAE – Tris-acetate/EDTA

TGS – Third Generation Sequencing

TMB – Tetramethylbenzidine

TSA – Tryptic Soy Agar

TSB – Tryptic Soy Broth

Table of Contents

1 Introduction 1
1.1 Marine ecosystem 1
1.1.1 The main marine habitats 1
1.1.2 The biological carbon pump 2
1.1.3 Marine benthic zone and the continental shelf 3
1.1.4 Benthic functioning and sediment-associated microbial communities 3
1.2 Important trace elements and minerals in the marine environment 4
1.2.1 Cobalamin 5
1.2.2 Cobalamin structure 5
1.2.3 Cobalamin analogs 6
1.2.4 Cobalamin-implicated microbial communities 6
1.3 Marine aquaculture 7
1.3.1 The environmental impacts of fish farming 8
1.4 Analytical methods 9
1.4.1 Polymerase Chain Reaction (PCR) and Quantitative PCR 9
1.4.2 Determination of microbial community composition via metagenomic analysis 11
1.4.3 Cobalamin measurement methods 12
Aim of the thesis 14
2 Materials and methods 15
2.1 Sample preparation 16
2.2 Preparation of the enrichment media - Bicarbonate-buffered synthetic crenarchaeota medium 16
2.3 DNA extraction for 16S rRNA gene sequencing 17
2.4 Library preparation of 16S rRNA amplicons for Illumina sequencing (MiSeq) 19
2.3 Quantitative measurement of bacterial and archaeal genome 21
2.4 Determination and quantification of cobalamin 22
2.4.1 Microbiological Assay 22
2.4.2 Enzyme-linked immunosorbent assay (ELISA) 23
2.5 Optimized protocol for parallel experimentation of ELISA and microbiological assay 24
2.6 Statistical analysis 25
2.6.1 Data processing of 16S rRNA Illumina sequencing data 25
2.6.2 Measurement of alpha (α) and beta (β) diversity 25
3 Results 26
3.1 Optimization phase for methods used in determining cobalamin 26

3.1.1 Optimization of Enzyme-linked immunosorbent (ELISA) assay for cobalamin detection ... 26
3.1.2 Optimization of microbiological assay for cobalamin detection ... 28
3.2 Determination and measurement of cobalamin using the optimized ELISA protocol ... 29
3.3 Determination and measurement of cobalamin using the optimized microbiological assay protocol ... 30
3.4 Quantification cycle (C_q) values from Quantitative PCR ... 31
3.4.1 Universal prokaryotic primers targeting the 16S rRNA gene's V3-V4 region ... 31
3.4.2 MCGI primers targeting the 16S rRNA gene's V3-V4 regions specific for ammonium-oxidizing archaea from the *Thaumarchaeota* phylum ... 32
3.5 Determination of microbial composition and diversity via 16S rRNA gene sequencing ... 33
3.5.1 Comparison of phylum composition between two oxygen conditions ... 33
3.5.2 Phylum composition of the sample uptakes ... 34
3.5.3 Genus composition ... 35
3.5.4 Alpha (α) diversity ... 36
3.5.5 Beta (β) diversity ... 37
4 Discussion ... 39
4.1 Microbial composition and diversity ... 39
4.2 Cobalamin abundance in enrichment media ... 41
4.3 Technical considerations for the assay optimizations ... 42
4.4 Limitations of the study and future perspectives ... 43
5 Conclusion ... 45
Bibliography ... 46
Supplementary materials ... 54
S.1 Index primers ... 54
S.2 Trace mineral components (100 mL) ... 54
S.3 Agar plates ... 55

1 Introduction

1.1 Marine ecosystem

Our home planet is vastly covered by a great body of saltwater. Land only accounts for a small proportion of the Earth's surface at approximately thirty percent, while the rest of the planet is submerged in water. With an average depth of 3730 meters (m), the ocean remains to be a mysterious conundrum, considering that a vast proportion of it is yet to be discovered and explored (Taksdal & Hågvar, 2001). It shelters multitude of species within the three domains of life: *Bacteria*, *Archaea*, and *Eukarya*; each enacting significant activities, functions, and interactions that frame marine life as it is. This is why marine ecosystems comprise of intrinsic multispecies synergies and interdependencies shaping the environment, and these ecosystems are sources of many services and goods that are beneficial to the planet and the whole biosystem. Services and goods include but are not limited to carbon sequestration, plant and animal resources, pollution control, habitats for breeding and nursery, raw materials, and livelihoods (Barbier, 2017).

Further, marine ecosystems are heavily defined by the unique ecological relationships between organisms, and their interactions with the present abiotic parameters such as sunlight, oxygen, temperature and many more. However, organic matter might be one of the most consequential abiotic factors that drives much of the ecological distribution and activities that occur in the ocean. This is because organic matter is a crucial component that fuels the concept of marine energy flow, the structure of the food web, and the sequestration of both nutrients and minerals in the ocean (Hansell et al., 2009; P.S. Kumar, 2021; Trombetta et al., 2020)

1.1.1 The main marine habitats

There exist two broad zones that classify the largest habitats in the ocean. The entire water column is also known as the pelagic, while the ecosystem found on the ocean floor is referred to as the benthic zone (P.S. Kumar, 2021). This division is important due to the dynamic interactions and exchanges that occur between the pelagic and the benthic zones. Much of the link between the water column and the ocean floor heavily involves energy in the form of organic matter and its transfer from either organism to organism or place to place. Organic matter is an important biological component as it contains nutrients and minerals necessary for organism growth and is a source of metabolic energy. Nitrogen, phosporus, sulfur, trace

minerals such as magnesium, iron, and cobalt, are just some of the essential components that are typically found in organic matter. In addition, it is the most dominant form of electron donor available in marine ecosystems. It is therefore crucial that this component is absorbed from the atmosphere and sequestered throughout the entire ocean including the sediments on the ocean floor (De La Rocha & Passow, 2014; Lønborg et al., 2020; Orcutt et al., 2011). There are two simultaneously occurring mechanisms that help fulfill these functions: the biological carbon pump and the microbial carbon pump (Dang, 2020; Polimene et al., 2017).

1.1.2 The biological carbon pump

The biological carbon pump is a mechanism comprising multiple processes by which diffusing inorganic carbon (i.e., carbon dioxide) absorbed by phytoplankton in the ocean's euphotic layer is fixed via photosynthesis and is exported all the way from the pelagic to the marine benthic zone as organic matter that is labile and bioavailable to other organisms (Dang, 2020; De La Rocha & Passow, 2014; N. Jiao et al., 2014). The exportation from the water column to the sediments can be achieved passively through the sedimentation of organic particles such as dead cells, fecal matters, and wastes from grazers feeding sloppily, or actively via vertical migration of planktonic communities and vertical downwelling of waters rich in organic matter (Claustre H. et al., 2021; N. Jiao et al., 2014; Nunnally, 2019; Polimene et al., 2017; Saba et al., 2011). During sedimentation, microorganisms also influence the efficiency of particle sedimentation by changing the organic matter composition through production of microbial Extracellular Polymeric Substances (EPS) on particle surfaces. This results in the total increase of the particles' total weight and its' susceptibility to gravity, ultimately promoting particle sedimentation (Decho & Gutierrez, 2017; N. Jiao et al., 2014; Passow, 2002). Unlike the biological carbon pump however, the microbial carbon pump, converts labile organic matter from phytoplankton into either its recalcitrant and/or semilabile forms. This means that organic matter derived from the microbial carbon pump is stored and is most often inaccessible to marine organisms. Though this mechanism plays little role in providing labile nutrients to the ecosystem, it is a mechanism vital for regulating the climate and the marine carbon pool, and sustaining microbial life (N. Jiao et al., 2014; Polimene et al., 2017). Both carbon-pumping mechanisms highlight the importance of microorganisms during the sequestration of energy in the entire ocean. However, the most influential microbial activity confined within these concepts might be the remineralization of the deposited organic matter. This is because a large proportion of the total dissolved organic matter deposited in the ocean is remineralized mainly

by heterotrophic bacteria. This influences the total respiratory flux of CO_2 back to the atmosphere and the release of bioavailable nutrients such as nitrogen, phosporus, and other bioessential trace minerals that are necessary for sustaining other marine organisms (Piontek et al., 2021; Wehrmann & Ferdelman, 2014).

1.1.3 Marine benthic zone and the continental shelf

In terms of spatial coverage, the marine benthic zone is considered as the largest ecosystem on the planet and plays a key role to many ecological functions in the ocean (Danovaro et al., 2017). It supports functional diversity, primary production, and plays a consequential part in the marine biogeochemical cycling and organic matter remineralization (Bremner et al., 2003; Covich et al., 2004; Danovaro et al., 2017; Snelgrove et al., 1997). The benthic zone is divided into different subzones based on depth. The intertidal zone (0-200 m), sublittoral zone (200-1000 m), bathyal zone (1000-4000), abyssal zone (6000-11000 m), and from 6000 m and below lies the hadal zone (P. Senthil Kumar, 2021). Relevant to the present study, the continental shelves within the intertidal zone cover approximately 9% of the ocean and comprise of marine ecosystems that serve as continental margins separating the land and the ocean. These include highly productive marine ecosystems such as esturaries, mangroves, salt marshes, and coral reefs (Alongi, 2020; Harris & Macmillan-Lawler, 2016). In terms of productivity, the continental shelf is more productive than the open ocean due to proximity to land, river runoffs, and a much deeper sunlight penetration that might promote photosynthetic activities all the way through the sediments (Sigman & Hain, 2012).

1.1.4 Benthic functioning and sediment-associated microbial communities

As particulate organic matter reaches the ocean floor, consumption by sediment-associated microbes and corresponsive metabolic pathways occur. Microbial abundance, activities, and biodiversity in benthic ecosystems, are greatly impacted by the export level of organic matter from the ocean surface (Danovaro et al., 2017). By the same token, phytoplankton within the sunlit zone are dependent on the fresh nutrients in the form of metabolic products from microbial remineralization in benthic ecosystems (Danovaro et al., 2017; Orsi, 2018). This dynamic exchange constitutes the significant coupling and interdependency between the pelagic and benthic ecosystems, in which microorganisms are the key variables.

Furthermore, the ocean, as depth increases, concentration of free oxygen becomes depleted, which is especially true when it comes to the benthic environment. Principally, the sediments

are divided into three layers depending on the environment's oxygen concentrations. In general, the first few meters of the sediment surface are oxygen rich and are thus referred to as the oxic layer. Below, the intermediate layer, where oxygen is present but is scarce, is called the suboxic layer, while the rest of the sediment below the former is the anoxic zone, where oxygen can no longer penetrate (Kristensen, 2000). Distinct and separate microbial communities are present within these confined zones, and this generates a sediment microbial and biogeochemical zonation controlled by the availability of specific terminal electron acceptors that subsequently influences the metabolic activities carried out in each sediment layer. In essence, this gradient in the sediments influences the microbial distribution, specific metabolic pathways, and the global biogeochemical cycling (Graw et al., 2018; Kristensen, 2000; Orcutt et al., 2011). For instance, in the oxic zone, oxygen (O_2) is the most thermodynamically favorable electron acceptor for microbial organic matter remineralization, thus sheltering an abundance of aerobic microbes. In the suboxic zone, the most dominant electron acceptor is nitrate (NO_3^-), while both nitrate and sulfate (SO_4^{2-}) dominate the deeper anoxic zone (Borges & Abril, 2011; Kristensen, 2000; Orcutt et al., 2011; Orsi, 2018). As these electron acceptors are consumed and metabolized for organic matter remineralization, recycling of corresponding nutrients occurs. Fundamentally, within the oxic region, nitrification is carried out as ammonium is oxidized by ammonium-oxidizing microbes to nitrate, while within the suboxic layer and the anoxic layer, denitrification processes are abundant (Frette et al., 1997; He et al., 2018; Pettersen et al., 2022; Ward, 2003). Furthermore, under anoxic conditions, electron acceptor such as sulfate is also abundant, thereby sulfate reduction occurs as well, which is an integral step in the sulfur cycle and is generally carried out by anaerobic sulfate-reducing microorganisms (Rabus et al., 2013; Simon & Kroneck, 2013).

1.2 Important trace elements and minerals in the marine environment

Trace elements are micronutrients that play key roles in the marine ecosystem. They function as enzyme cofactors that help catalyze enzymatic reactions in many essential metabolic pathways (McElroy & Swanson, 1953; Morel et al., 2003). Manganese (Mn), iron (Fe), cobalt (Co), nickel (Ni), copper (Cu), and zinc (Zn) are some of the most important trace elements in the ocean, and most often, their supply can be biolimiting (Morel, 2000). This is because their metabolic functions can determine the rates of the primary productivity in the ocean (Jia et al., 2020). For instance, the trace element iron is an indispensable micronutrient in the ocean because of its roles in the phytoplankton's photosynthetic transport chain and as an integral

component in enzymes involved in nitrate assimilation (Schoffman et al., 2016). Regulation of biological productivity is not limited to iron as other trace elements also play separate, yet crucial roles in regulating primary production (Jia et al., 2020).

1.2.1 Cobalamin

The metabolic activities of respiring and fermenting microbes within benthic environments are also fundamental for the biosynthesis of essential biological components, and not just its' sequestration. Specifically, the distribution of the trace mineral, cobalt, which is integral in terms of microbial production of a biologically significant coenzyme, cobalamin (Osman et al., 2021). Primarily, cobalamin is utilized as a catalyzator by many prokaryotic and eukaryotic organisms during methyl-transfer activities. These include cellular activities such as amino acid synthesis (i.e., cobalamin-dependent methionine synthase), circulation of carbon via the Krebs cycle (i.e., adenosylcobalamin-dependent methylmalonyl-CoA mutase), and most importantly, DNA synthesis (i.e., ribonucleotide reductase) (Doxey et al., 2015). Despite its vital roles in both eukaryotic and prokaryotic cells, however, it is considered essential. This means that most marine microorganisms have no genetic capacity to synthesize cobalamin (cobalamin auxotrophs) and are therefore reliant on those who can (cobalamin prototrophs) (Wienhausen et al., 2022). Cobalamin is therefore a rate-limiting component for marine primary production and the cellular growth of many cobalamin auxotrophs (Heal et al., 2017; Helliwell et al., 2016). The interdependency between the cobalamin-auxotrophs and prototrophs is therefore based on the mutualistic exchange in which the auxotrophs are provided with cobalamin, and correspondingly, organic nutrients are obtained by the prototrophs (Heal et al., 2017).

1.2.2 Cobalamin structure

Cobalamin, among all the vitamins, is the largest and most complex. It consists of a corrinoid ring with a central cobalt-ion, a lower ligand of a compound called 5,6-dimethylbenzimidizole (DMB), and an upper ligand of either methyl (Me-), adenosine (Ado-), cyano (CN-), or a hydroxy (OH-) group (Heal et al., 2017; Osman et al., 2021). Moreover, its complex structure reflects the intricate biosynthesis of the coenzyme that comprises roughly thirty enzyme-mediated steps (Raux et al., 2000).

1.2.3 Cobalamin analogs

Methylcobalamin, adenosylcobalamin, and hydroxocobalamin are cobalamin analogs that are naturally occuring, whereby cyanocobalamin is synthetic (Balabanova et al., 2021), specially made for human consumption, as in clinical purposes and supplements. Methylcobalamin (MeCbl) is used in various methyl-transfer reactions such as the methylation of homocysteine to produce methionine, which is integral for DNA and protein synthesis (Oohora & Hayashi, 2016). Utilization of adenosylcobalamin (AdoCbl/coenzyme B_{12}) on the other hand, is fundamental to the degradation of various amino and fatty acids, as well as the synthesis of thymidylate, which is a key component in DNA synthesis (Helliwell et al., 2016; Tsiami & Obersby, 2017). There exists, however, an analog of cobalamin that has the same abundance in natural marine systems, namely the pseudocobalamin, which is primarily biosynthesized by most, if not all members of *Cyanobacteria*. The main differences between cobalamin and pseudocobalamin are the α ligands in which the latter consists of an adenosine molecule instead of DMB, and its bioactivity, since pseudocobalamin is, in principle, to most microorganisms, biologically unavailable (Grossman, 2016; Heal et al., 2017; Helliwell et al., 2016). Nonetheless, recent studies suggests that some microalgal species and bacteria display species-specific features that if provided with DMB, can remodel pseudocobalamin to cobalamin, using the enzyme cobalamin synthase (CobS), as well as salvage an intermediate molecule, cobinamide, to produce cobalamin. This is especially true for the cases of diverse *Vibrio* species that carry out partial biosynthetic pathways for cobalamin (Grossman, 2016; Helliwell et al., 2016; Ma et al., 2020).

1.2.4 Cobalamin-implicated microbial communities

De novo biosynthesis of cobalamin is confined to a limited list of *Bacteria* and *Archaea*. *Cyanobacteria*, *Alphaproteobacteria*, *Gammaproteobacteria*, *Bacteriodetes*, *Euryachaeota*, *Crenarchaeaota*, and *Thaumarchaeota* are among the taxa which have cobalamin-producing members (Doxey et al., 2015). However, in terms of genomic potential and abundance, *Thaumarchaeota* might be the most globally significant cobalamin producer in the marine environment (Doxey et al., 2015; Heal et al., 2017).

1.2.4.1 Thaumarchaeota as the major de novo biosynthesizers of cobalamin in the ocean

Thaumarchaeota is a phylum that belongs to the *Archaea* domain. The phylum largely consists of ammonia-oxidizing organisms, and the majority of these archaea perform the first step of nitrification, in which conversion of ammonia to nitrite occurs using the enzyme ammonia monooxygenase (AMO), thus are key in the marine nitrogen cycling (Stieglmeier et al., 2014). High presence of *Thaumarchaeota* can be observed in the surfaces of oxic deep-sea sediments. They use both ambient ammonia and those released by heterotrophic organisms, especially from microorganisms, to fuel their primary production and carbon fixation, sustaining the benthic seafloor with autotrophic metabolism (Doxey et al., 2015; Orsi, 2018; Pinto et al., 2020). *Thaumarchaeota* species display oligotrophic metabolism as well, meaning that they have the capacity to thrive in low nutrient environments (Doxey et al., 2015). This phylum is ecologically important on account of its abundance in the marine environment, as it represents ~20% of all marine prokaryotes, is the most abundant Archaea in the Earth, and its implication in cobalamin-synthesis (Doxey et al., 2015; Heal et al., 2017). Select *Thaumarchaeota* species are major producers of cobalamin, particularly, the genus *Nitrosopumilus* (Heal et al., 2017; Pinto et al., 2020). Several studies involving the archeon *Nitrosopumilus* maritimus SCM1 revealed that this species and in fact, all known ammonia-oxidizing archaea such as Candidatus *Nitrosopumilus salaria* and Candidatus *Nitrosopumilus koreensis* AR1 all share genetic markers for cobalamin biosynthesis pathway, and thus have the genetic capacity to produce cobalamin (Doxey et al., 2015; Law et al., 2021).

1.3 Marine aquaculture

Marine aquaculture is an industry in which marine organisms, most particularly fish, are cultivated, nurtured, and harvested. This can be done either offshore or within enclosures (Laird, 2001). Contemporarily, it is the most rapid growing sector within the food industry, contributing a large proportion of the global fish food (Pikelj et al., 2022). The rapid growth of aquaculture can be attributed to multiple socioeconomic drivers including the ever-increasing demand for food supply caused by the global population's rapid increase, a drastic yield decline from wild fisheries, and the goal to reduce global reliance on wild fish resources (Fiorella et al., 2021; Frankic & Hershner, 2003; Naylor et al., 2021). In addition, products yielded by marine aquaculture comprise of major sources of protein beneficial for human consumption (Ahmad et al., 2021). Furthermore, the development of this industry could provide potential solutions for improved food security, especially in developing countries. In addition to food security, the

socioeconomic advantages expand to job security, production of fish that are more affordable to the masses due to production efficiency, reducing the strain on overexploited natural resources and wild stocks, providing a profitable crop, and the list goes on (Ahmad et al., 2021; Williams, 1999).

One of the largest aquaculture exporters in the world is Norway. In the early 1970s, Norway pioneered the sea-cage farming of Atlantic salmon (*Salmo salar* L.) and is currently one of the largest and most profitable export industries of the country (Taranger et al., 2014). In 2015, 53% of the world's Atlantic salmon production derived from Norway. Housing about 400 watercourses abundant with Atlantic salmon, its farming is therefore significant in the Norwegian industry considering that it also generated approximately 6000 jobs and contributes heavily to the country's GDP (Olaussen, 2018).

1.3.1 The environmental impacts of fish farming

Despite the benefits, harmful environmental impacts caused by fish farming are becoming more and more apparent. Globally, marine aquaculture sites are situated near the shore or within coastal ecosystems such as estuaries and mangrove forests (Polidoro et al., 2010; Valdemarsen et al., 2012). Both of which provide various ecosystem services including but not limited to nursery for diverse organisms, carbon sequestration, and nutrient provision for many aquatic species (Abu El-Regal & Ibrahim, 2014; Polidoro et al., 2010). Demolition of these natural habitats is done in order to build aquaculture sites, consequently abolishing its ecosystem services (Polidoro et al., 2010). However, another significant environmental impact occurs at the bottom of the ocean which, to a great extent, affects the biogeochemical functioning of the benthic ecosystem (Keeley et al., 2019; Valdemarsen et al., 2012; Williams, 1999).

Marine benthic degradation due to large-scale, intensive fish farming has gained much attention in the past few years as the rapid growth of marine aquaculture continues to propel. This is due to the extremely high sedimentation rates that occur within the sea cages. The intense sedimentation of organic waste derived from large amounts of both fish feed and fish excretion to the seafloor might be the most significant contributors to benthic malfunctioning. This is because sulfate-reduction and methanogenesis can be promoted and result in the accumulation of toxic compounds such as sulfide (S^2) and methane (CH_4), both of which can lead to the loss of microbial and macrofauna activities such as remineralization of carbon, ventilation, and burrowing activities (Valdemarsen et al., 2012). In addition, regions that are subject to heavy sedimentations experience oxygen depletion due to the increase in microbial metabolic

activities (Orsi, 2018; Xu et al., 2022). Further, the localized metabolic waste from thousands of fish and their feed are rich in nitrogen and phosphorus, by which excessive input can also lead to eutrophication and oxygen depletion (Chislock et al., 2013; Lazzari & Baldisserotto, 2008). Consequently, as oxygen, the optimal terminal electron acceptor in oxic regions, becomes scarce in the environment, a shift from oxic to anoxic respiration is most likely to occur (Orsi, 2018; Pettersen et al., 2022; Xu et al., 2022). In anoxic conditions, accumulation of toxic gases including hydrogen sulfide (H_2S) is prominent (Pettersen et al., 2022). These habitat modifications can lead to loss of microbial diversity and ultimately lead to mass mortality events in sea-cages and/or the marine coastal environment (Chislock et al., 2013; Pettersen et al., 2022).

In Norway, the rapid expansion of sea-cage farms distributed along the Norwegian coastline, is a cause for environmental concerns due to the potential negative effects of the industry to the marine ecosystem (Taranger et al., 2014). It has been reported that eutrophication in the fjords due to sinking undigested feed and feces derived from the fish farms, were equivalent to sewage release of 10 million people. Further, in 2015 phosphorus release in the fjords from aquaculture was almost fifty times higher than the whole Norwegian industry. Moreover, nitrogen emission from fish farms surpassed the country's industry by twenty-four times in 2014 (Olaussen, 2018). As mentioned, the probability of developing eutrophication increases when the levels of both nitrogen and phosphorus are elevated. This was evident in May 2019 where a constant algal bloom within fish farms in the Norwegian northern coast resulted in over eight million salmon suffocating and dying (Magra, 2019).

1.4 Analytical methods

1.4.1 Polymerase Chain Reaction (PCR) and Quantitative PCR

Polymerase Chain Reaction or PCR is a tool used to exponentially amplify a target sequence within a DNA template. Aside from the DNA template, the main components in a PCR are the following: primers that are designed specifically as complements for the prime ends of the target sequence, DNA polymerase (thermostable), and dNTPs (deoxynucleotide triphosphates) (Bhatia & Dahiya, 2015; Canene-Adams, 2013). PCR consists of three fundamental steps that are repeated in cycles: denaturation, annealing, and extension. Essentially, the first step is performed to separate the two strands of the DNA at 94°C. In the annealing step, the strands are cooled down to 52°C. This allows for the forward and reverse primers to bind to the prime

ends of the target sequence on the separate strands. During the extension process, nucleotides bind to complementary bases on the template strands, which is a process catalyzed by the thermostable DNA polymerase at 72°C. This cycle is repeated and amplifies the target sequence at an exponential rate (Bhatia & Dahiya, 2015). The most common applications of PCR include, but are not limited to, detecting pathogenic microorganisms, diagnosing diseases that are genetic, paternity testing, and study of gene expression (Lenstra, 1995).

PCR is often coupled with another technique referred to as the agarose gel electrophoresis. This method is used to separate DNA fragments according to their size and charge. PCR amplicons, often premixed with a specific loading dye, are applied in the wells of the agarose gel that is slightly submerged in a buffer consisting of Tris-acetate/EDTA (TAE). The electrophoresis equipment in which the agarose gel and the buffer is put into has a negatively charged cathode and a positively charged anode. Due to the phosphate backbone of DNA, it has an overall negative charge and when electrical current is run through the gel, DNA will move towards the anode. The distance by which DNA fragments will travel would vary, mainly due to the molecular weight of each fragment. Smaller fragments will cover larger distances while larger ones will travel shorter distances. Often, a DNA ladder is applied to the gel to be used as a reference to estimate the fragments' size or distance travelled. After separation, UV light is used to visualize the fragments (Lee et al., 2012). For the present study, the technique was used to verify DNA abundance within the samples.

Quantitative PCR is an alternative amplification method based on the principles of PCR. In the conventional PCR, amplicon and abundance are difficult to detect without using methods such as agarose gel electrophoresis for visualization. In qPCR, detection occurs in real time, as each amplification cycle is monitored using fluorescent signals by adding fluorescent dyes or fluorescently labelled probes. In qPCR, the concentration of the target sequence must be above a detectable threshold to be quantified and is monitored in terms of quantification cycles (C_q), which is the point at which the concentration can be detected (Kralik & Ricchi, 2017). Principally, low C_q values or earlier detection indicate a high concentration of the target sequence, while low concentrations are detected at later cycles, represented by a high C_q value.

1.4.2 Determination of microbial community composition via metagenomic analysis

1.4.2.1 Ribosome and the 16S rRNA gene

The ribosome is an organelle that can be found in every living organism. It is the cellular component that carries out the translation of genetic codes into proteins, a process also known as protein synthesis (Rapin et al., 2017). In addition, they are made up of both proteins and ribosomal ribonucleic acid (rRNA) and they consist of two subunits that can be distinguished by size, a larger subunit and a smaller subunit. The 80S ribosome of eukaryotes contains two subunits. The 60S large subunit contains the following rRNA molecules: 28S, 5S, and 5.8S rRNA, while the small subunit contains the 18S rRNA. On the other hand, the prokaryotic ribosome, also known as the 70S ribosome, contains a large and a small subunit as well. Referred to as the 50S ribosome, the large subunit contains the 5S and the 23S rRNA molecules, while the 30S small subunit contains the 16S rRNA molecule (Bhavsar et al., 2010). In metagenomic studies involving bacterial and archaeal taxonomic classification, the 16S rRNA is the most commonly used marker. This is because they consist of extremely conserved gene structure and sequence, as well as species-specific hypervariable regions (V1-V9) (Raina et al., 2019; Rapin et al., 2017).

1.4.2.2 Next-generation sequencing of the 16S rRNA gene

There are several methods used to sequence the 16S rRNA gene. The Sanger sequencing, Next-Generation sequencing (NGS), and the Oxford Nanopore Sequencing are three of the main 16S rRNA sequencing technologies available to date (Santos et al., 2020). The Sanger sequencing was responsible for most of the gathered data on metagenomics, providing high quality and long read lengths stretching from 400-900 basepairs, but the system is low-throughput, time- and labor intensive, and not cost-efficient (Petrosino et al., 2009; Santos et al., 2020).

The Next-Generation Sequencing (NGS), also known as the Second-Generation sequencing encompasses alternative sequencing systems but almost all comprise of a similar concept and workflow. One of the most utilized NGS approaches is the Illumina system which applies the principle of sequencing by synthesis (SBS). This system's workflow comprises of the following steps: library preparation, cluster generation, sequencing, and ultimately, data analysis (Inc., 2017; Shendure & Ji, 2008). The library is prepared through a series of steps following the Illumina protocol. Then, as the sample is loaded to the flow cell, DNA fragments attach to the flow cell's surface and become clonally amplified through bridge amplification,

ultimately, generating clusters of DNA template strands. Subsequently, sequencing is initiated through the extension of the DNA templates by a reversible terminator-based method. More specifically, a single fluorescent-tagged ddNTP (dideoxynucleotide triphosphates) attaches to the DNA templates while simultaneously hindering the attachment of other ddNTPs, ensuring that only one nucleotide is incorporated at a time. As the ddNTPs become incorporated during the extension process, nucleotide-specific fluorescent signal is emitted and is identified during sequencing. The last step for the Illumina system is data analysis in which the sequenced reads are aligned and compared with a reference genome of choice. There are many possible analytical approaches that can be used including but not limited to insertion-deletion (indel) identification, single nucleotide polymorphism (SNP), phylogenetic analysis, and metagenomic analysis (Inc., 2017; Shendure & Ji, 2008).

In general, NGS systems such as Illumina provide high-throughput sequencing of high quality and are time- and cost-efficient. However, they generate short reads that are generally much shorter than Sanger sequencing (Mestan et al., 2011). In effect, it became a must to use specialized tools for bioinformatics and intricate post-processing pipelines (Athanasopoulou et al., 2022). Attempting to provide a solution for the short read disadvantage, emerging systems belonging to the Third Generation Sequencing (TGS) or long-read sequencing such as PacBio and Oxford Nanopore's MinION are therefore becoming more and more prevalent (Rhoads & Au, 2015). These platforms offer enhanced sequencing chemistry, thus generating production of long reads that allow for better reconstructions of genome compared to NGS. In addition, TGS systems perform both single-molecule sequencing and real-time sequencing that permits less bias and enhanced homogenous genome coverage opposed to NGS (Athanasopoulou et al., 2022; Rhoads & Au, 2015).

1.4.3 Cobalamin measurement methods

There are various methods to determine the abundance or measure the concentration of cobalamin within a system. These include, but are not limited to, microbiological assay by agar cultivation method, ELISA (enzyme-linked immunosorbent assay), High-performance liquid chromatography (HPLC), Radioimmunoassay (RIA), homocysteine test, and nitrite (N_2) measurement. Out of all these methods, ELISA and microbiological assay were the least complex and the most adaptable measurement methods and were therefore the primary approaches performed for the present study.

1.4.3.1 Enzyme-linked Immunosorbent Assay (ELISA)

Enzyme-linked immunosorbent assay or ELISA is a simple and sensitive technique principally used to quantify the abundance or determine the presence of a specific soluble substance such as antigens, antibodies, proteins, or vitamins in a sample (Butler, 2000; Reen, 1994). This technique is widely used for diagnostic purposes, but it can be applied to various objectives. Essentially, ELISA heavily involves enzyme-coupled antibodies that can attach to the antigen in the given sample. The antibodies are highly specific and will only bind the antigens they are designed to attach to. There are four main types of ELISA, direct, indirect, sandwich, and competitive ELISA. In competitive ELISA, specific antigens are bound to the bottom of the container. A serum containing an unknown concentration of antibodies specific to the bound antigens is added to the container. Addition of enzyme-linked antibodies that are also specific to the bound antigens is performed as well. The enzymes that are linked to the antibodies react to chromogenic substrates. After incubation, a strong acid is typically added to stop the reaction. The presence of the serum antibody is then determined by the color intensity of the solution following the competition between the serum antibodies and the enzyme-linked antibodies. A positive or a highly concentrated result would result in a colorless solution, while a pigmented solution indicates a negative result or a serum with low concentration of the antibody (Alhajj et al., 2023; Sakamoto et al., 2018). A commonly used approach to determine this is spectrophotometry via plate readers to obtain the absorbance measurement of the solution (Hayrapetyan et al., 2023).

1.4.3.2 Microbiological assay

Another technique to determine the concentration of a certain compound is microbiological assay. In this method, susceptible microorganisms are used to determine the effects of the compound of interest on microbial growth. Compounds such as vitamins, amino acids, and antibiotics are typically used in this context as they are biologically reactive. Two of the most used approaches are the agar diffusion and the tube methods. In the present study, agar diffusion was used, and, in this approach, the susceptible microorganism can be seeded with the agar medium or a small suspension volume of the cultivated microorganism on the agar surface can be applied. The compound of interest can then be applied in different ways. A widely used approach is the use of sterile filter paper disks that have been exposed to the compound of interest prior to application on the agar surface. After incubation, the effects and potency of the compound can be empirically measured via measurement of either growth or inhibition zones (Hewitt, 1977a, 1977b).

Aim of the thesis

The present study was conducted under the hypotheses and observations obtained from Pettersen et al. (2022). It was hypothesized that cobalamin might be a key component in sustaining high species richness. Consequently, the authors' observations illustrated that there were strong correlations between ammonium-oxidation and high microbial diversity (high OTU), while denitrification and high levels of both nitrate and organic carbon were positively associated with low microbial diversity (low OTU). In addition, their results showed that there was a strong association between high microbial diversity in the benthic environment and the abundance of the cobalamin-implicated archaeon, *Nitrosopumilus*. They predicted therefore that cobalamin could be associated with high microbial diversity as well.

Therefore, the aim of the thesis is to investigate the effect of adding a combination of nitrate and organic carbon in the form of succinate and sulfate and succinate on both the microbiota composition and the concentration of cobalamin on marine sediments. To achieve this, the following subgoals were set:

- Establish simple approaches to measure cobalamin and optimize the methods
- Perform a microcosm pollution experiment (enrichment) to investigate the impact of the following component combinations on benthic microbial diversity:
    - Ammonium (no succinate)
    - Sulfate + succinate
    - Nitrate + succinate
- Enrich and cultivate the genus *Nitrosopumilus* within the ammonium-oxidizing media
- Measure cobalamin from the initial and final set of sediment samples
- Identify microbial composition from the set of sediment samples retrieved during the microcosm pollution experiment

2 Materials and methods

The "Optimization phase" was done in parallel with the microcosm pollution experiment. Then, two categories of conditions were set for the microcosm pollution experiment: oxic and anoxic. The following media was then created: an ammonium-oxidizing, nitrate-reducing, and a sulfate-reducing medium. Each medium was divided into two and were placed under the set conditions. A total of nine times were the number of sample collections performed over the course of four weeks (T0 – T8). Three of the initial (T0) samples (n = 6) retrieved from the Hvitsten bay were used for ELISA and microbiological assay (n = 3), while the remaining half (n = 3) were used as controls for the metagenomic analysis. Meanwhile, the extra samples (n = 18) that were retrieved during the last sample collection (T8) were also used for ELISA and microbiological assay. All samples (n = 144) collected during the four-week period (T1-T8) were utilized for DNA extraction and consequently, for qPCR, 16S rRNA library preparation, and MiSeq sequencing. Chief engineer, Inga Leena Angell, performed the last stage of the library preparation and the data processing of the results generated from the 16S rRNA sequencing data. Below is a figure that illustrates the synopsis of the experimental design, as well as an overview of the divided set of samples and experimental procedures used in the present study.

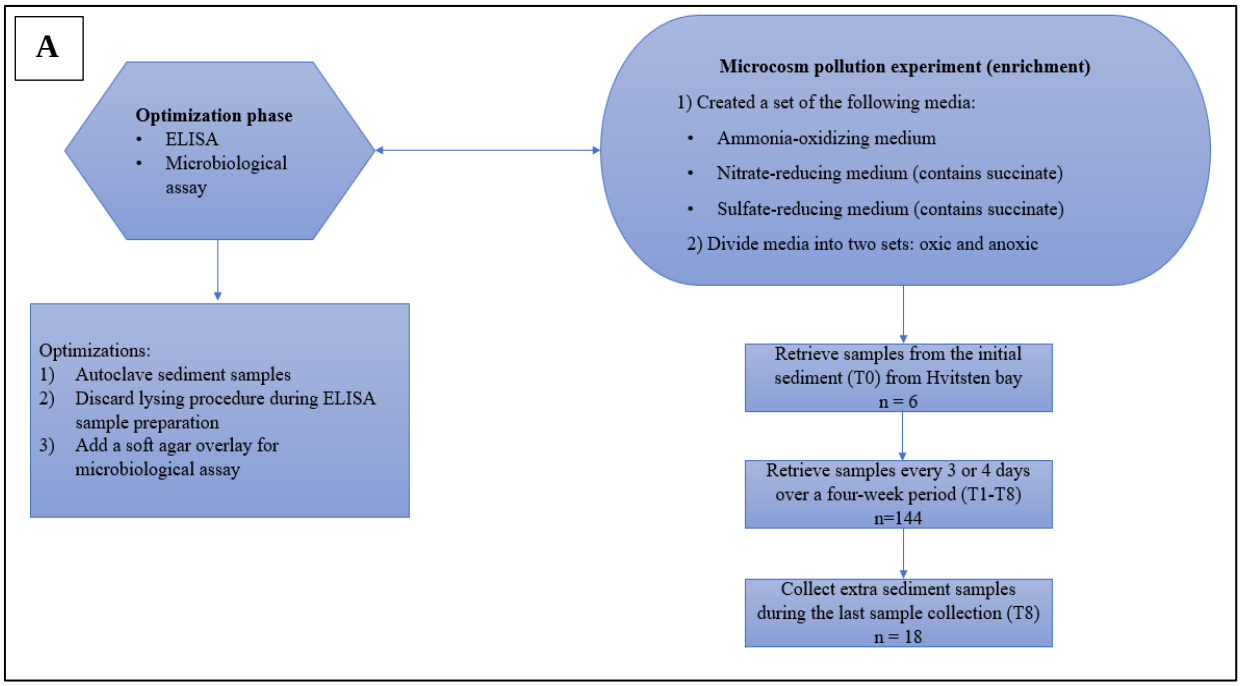

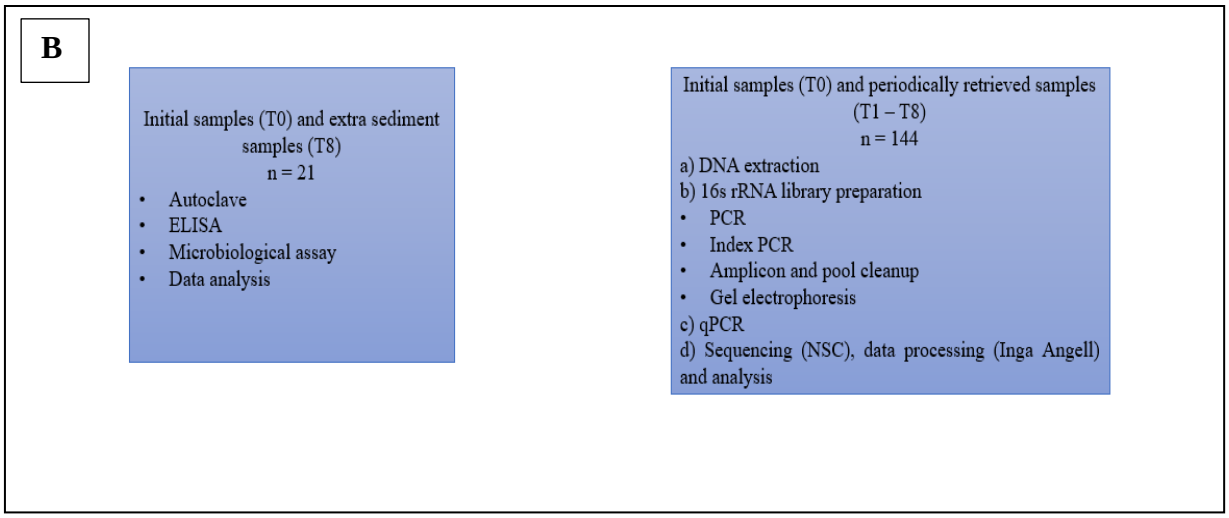

Figure 1: Flow chart illustrating the experimental design for the present study and an overview of the experimental procedures that were performed on the divided datasets. A) illustrates the experimental workflow of the present study, and B) shows the division of datasets as well as the corresponding experimental procedures that were performed on the samples. The last step of 16S rRNA library preparation and data processing was performed by Chief Engineer, Inga Leena Angell, which consisted of quantification of amplicons in the pooled library. The sequencing was done using a Miseq instrument and the Miseq Reagent Kit v3 (600-cycle) and was performed in the Norwegian Sequencing Center (NCS) in Oslo.

2.1 Sample preparation

At three meters, sediment samples were retrieved from the Hvitsten bay in Vestby municipality and were distributed among 500 mL beakers along with 300 mL of the specific enrichment medium accordingly. All beakers were covered with aluminum foil. Some were enclosed in a ten-liter anaerobic chamber, while the others were placed under normal incubation conditions. Anaerogen (3.5 L) packs (Thermo Fisher Scientific, USA) were placed in the anaerobic chamber, as well as anaerobic indicators to ensure an anoxic environment. All beakers were then incubated in a refrigerator at 10°C to simulate the average marine temperature.

2.2 Preparation of the enrichment media - Bicarbonate-buffered synthetic crenarchaeota medium

Three enrichment media were prepared for the experiment, which all consisted of the following components: 78g NaCl, 15g $MgSO_4*7H_2O$, 15g $MgCl_2*6H_2O$, 4.5g $CaCl_2*H_2O$, 0.3g KBr, and approximately 3000 mL MilliRo water. These components were adapted from Diding (1951) The 3-liter medium was divided into three 1L containers and were all autoclaved at 121°C for

15 minutes. After cooling, the following solutions were added aseptically using 0.2 µm filters and 10 mL syringes: 3 mL $NaHCO_3$ [1M], 5 mL KH_2PO_4 [0.4 g/L], 1 mL FeNaEDTA solution [7.5 mM], 1 mL trace element solution (Supplementary material S.2), and 0.1 mL alpha-ketoglutaric acid (100 mM). Three following medium were then created:

a) 0.2 mL NH_4Cl was added aseptically to create the ammonium-oxidizing medium
b) 3 g succinic acid and 2 g $NaNO_3$ was aseptically added to create the nitrate-reducing medium
c) aseptically added 3 g succinic acid to create the sulfate-reducing medium.

Enrichment and sample collection

Initial sediment samples (T0) were collected and stored into Sarsedt scoop containers, in which some contained 3 mL of Stool Transport and Recover buffer (S.T.A.R.) each and were stored in the freezer at -20°C, while the rest solely contained sediments that will be used for ELISA and microbiological assay.

Sediment samples were taken from each beaker every three or four days over the course of four weeks and were placed in prepared Sarsedt containers containing 3 mL of S.T.A.R. buffer and were frozen at -20°C. Renewal of Anaerogen packs and indicator swabs were also performed for each time a sample taking has occurred. At the last sample taking (T8), extra sediment samples were retrieved from the beakers for future use in ELISA and microbiological assay.

2.3 DNA extraction for 16S rRNA gene sequencing

Sample lysis

Sample lysis was achieved using the last sediment samples that were retrieved from the beakers and the Zymo Research QuickDNA™ Fecal/Soil Microbe 96 MagBead kit. The Sarsedt scoops containing the sediments were vortexed briefly for 15 seconds each. Samples were then added to prepared BashingBead Lysis tubes by cutting the bottom part of the pipette tips to ensure that sediments were retrieved. Next, 750 µL Lysis Solution (Bashing Bead Buffer) was added to each tube followed by further addition of 100 µL EDTA [0.5M] and 100 µL Sodium Citrate [0.5M]. The samples were mechanically lysed using the TissueLyser (Qiagen, USA) at maximum speed for 2x2.5 minutes to disrupt the cell wall and to consequently release nucleic acid into the lysate. Then, the lysates were centrifuged at 13000 rpm for 3 minutes to form a pellet containing cellular debris that may cause unwanted reactions during the DNA extraction.

DNA extraction

The extraction of DNA was done automatically using the KingFisherFlex (Thermo Fisher Scientific, USA) robot and was initiated with the transfer of 200 µL of the supernatant from the lysed samples to the wells of a 96 DW sample plate. Then, 600 µL of Quick DNA Mag Binding Buffer was added to each well followed by the addition of 25 µL Mag Binding Beads, which are both used to selectively bind DNA to the silica beads using silica-binding chemistry utilizing the high salt conditions provided by the buffer. Next, other plates were prepared. The tip plate was filled with the 96 DW Tip comb, the PreWash plate with 900 µL of Pre-Wash buffer into each well, 900 µL of gDNA Wash buffer into Wash plate 2 and 3. Washing steps are necessary to remove contaminants in the lysates. The last plate, the Elution plate, was filled with 60 µL Elution buffer into each well by which DNA becomes released from the binding beads into the solution. The retrieved eluted DNA was then stored at -20°C for future use.

Measurement of DNA quantity by Varioskan and Qubit

The concentration of DNA was measured using two parallel methods. First, the 2 µL template DNA was aliquoted into each well of a 96 flat bottom NUNC well. Then prior to putting the plate into the Varioskan LUX plate reader, 70 µL Quant-iT™ Working Solution was added into each well containing the template DNA and was gently mixed by pipetting up and down ten times and letting the reaction occur in the dark for a minute. After retrieving the relative fluorescence units (RFU) from the plate reader, select samples of varying RFU, preferably from highest to lowest, are chosen as template for a standard curve through which DNA concentrations from each well can be estimated. To perform this, the protocol "Quant-iT™ Assays Abbreviated Protocol (Invitrogen Corporation, 2007) and a Qubit Fluorometer (Invitrogen, USA) were used. In each Qubit tubes, 2 µL template DNA and 198 µL Quant-iT™ Working Solution were added and mixed. Then the tubes were vortexed for 10 seconds each and were incubated at room temperature for one minute in the dark. After brief incubation, the tubes were placed in the Qubit Fluorometer (Invitrogen, USA) using the program "High-sensitivity dsDNA" to quantify the DNA concentration of each template DNA.

2.4 Library preparation of 16S rRNA amplicons for Illumina sequencing (MiSeq)

First stage PCR (Amplicon PCR)

The PCR reaction mix consisted of the following components: 5X HOT FIREPol® Blend Master Mix Ready to Load (origin), 0.2 µM Forward (341F) and Reverse (806R) primers (Table 1), Nuclease-free water, and 2 µL template DNA, which had a total volume of 25 µL in each well. The plate was then put for a spin using the plate spinner for 20 sec. The PCR amplification program on the 2720 Thermal Cycler (Applied Biosystems, USA) that was used is as follows: One cycle of 95℃ for 15 min, 25 cycles of 95℃ for 30 sec, 55℃ for 30 sec, 72℃ for 45 sec, a cycle of 72℃ for 7 min, and the remaining time at 10℃ for ∞. Then a PCR amplicon clean-up was performed followed by gel electrophoresis.

Agarose gel electrophoresis

After amplification, the PCR amplicons are be loaded in a prepared 1%-2% agarose (Invitrogen, USA) gel that contained 1x tris-acetate EDTA (TAE) buffer (Invitrogen, USA), in which PeqGreen dye (Peqlab, Germany) was added as a pigmenting component. In each amplicon loading, a PCR DNA ladder with the size of 100 bp was loaded which displayed bands used as DNA length references. In the present study, 70V for 40 min was the program used for the gel electrophoresis equipment containing 1x TAE-buffer. Next, the gel is retrieved from the equipment after electrophoresis and was put in the Molecular Imager Gel Doc™ XR Imaging System (BioRad, USA) for UV visualization.

Clean up of PCR amplicon

PCR amplicon clean-up was done manually using 1x Sera-Mag Speed Beads solution. The Sera-Mag beads selectively bind DNA from the PCR product and using a magnetic stand, the beads become isolated from the supernatant along with the DNA. After a series of washing steps using 80% ethanol, the supernatant was discarded, and the beads were left to be air-dry for 15 minutes. Next, Nuclease-free water was gently mixed to the beads in order to unbind the DNA from the beads. After bead isolation using the magnets, the supernatant was retrieved containing purified DNA.

Index PCR

The purified DNA was used as the DNA template for Index PCR which was performed automatically by the Eppendorf epMotion 5070 robot (Eppendorf AG, Germany). First, different combinations of forward and reverse primers were set up, whereas each combination

was made sure to be present only once. This is to ensure that every single sample would have a unique index for future use in 16S Illumina sequencing. The Index PCR reaction cocktail contained the following components: 5x FirePol® Master Mix Ready to Load, 0.2 µM Forward (F1-F8) and Reverse primers (R1-R23) (Supplementary material, S.1), Nuclease-free water, and the purified DNA as the template. The final volume achieved for each reaction is 25 µL. After spinning the plate for 20 sec, the fragments were amplified using the following program on: one cycle of 95℃ for 5 mins, 10 cycles of 95℃ for 30 secs, 55℃ for 1 min, 72℃ for 45 secs, one cycle of 72℃, and 10℃ for ∞. After amplification, gel electrophoresis and UV visualization using the Molecular Imager Gel Doc™ XR Imaging System (BioRad, USA) were performed.

Quantification and Normalization

During this step, the same methods were performed as measuring the DNA concentration of PCR amplicons, only this time, the template DNA used were amplicons obtained from the Index PCR. Quantification is performed using the VarioSkanLUX (Thermo Fisher Scientific, USA). Once the RFU data were obtained, specific samples ranging from highest to lowest RFU value were selected for creating a standard curve by which DNA concentrations in each amplicon can be estimated. The selected samples were aliquoted to Qubit assay tubes and were ran in the Qubit Fluorometer (Invitrogen, USA) and concentration in ng/mL were obtained, and using these results, a standard curve was generated.

Based on the sample with the highest concentration, the remaining samples were then normalized. This was done to calculate the volume needed from each sample during sample pooling. Due to the requirements specified in the protocol for the robot, Biomek 3000 (Beckman Coulter, USA), anything more than 10 µL or less than 1 µL were negligible and were set to a specific amount depending on the overall cut off concentration. After pooling all the samples in a single 5 mL Eppendorf tube, DNA concentration was measured using the methods for Qubit Fluorometer (Invitrogen, USA).

Clean up of pooled library

A clean up procedure was performed on the pooled library using 0.1% Sera Mag Speed Beads Solution (0.8X µL). The magnetic beads, like the first clean up, were designed to selectively bind DNA products and isolate them from the supernatant through the magnetic stand. After the washing steps, the beads were added with Nuclease-free water and was gently mixed. Then, the beads were put in the magnetic stand to isolate them from the supernatant, which contained

the purified DNA. The supernatant was then transferred to a sterile 1.5 mL Eppendorf tube and was sent for sequencing after measuring concentration using the Qubit Fluorometer (Invitrogen, USA).

2.3 Quantitative measurement of bacterial and archaeal genome

Quantitative PCR (qPCR) targeting 16S rRNA V3-V4 region using universal primers

The following components were mixed together to create the qPCR reaction mix: 5x HOT FIREPol® EvaGreen® qPCR supermix, 0.2 µM Reverse (806R) and Forward (341F) primers (Table 1), Nuclease-free water, and the template DNA (eluted DNA from DNA extraction) which had a total volume of 20 µL. The amplification of the PCR product was performed using the C1000 Touch™ Thermal Cycler (BioRad, USA) and the following program: one cycle of 95℃ for 15 mins and 40 cycles of 95℃ for 30 secs, 55℃ for 30 secs, and 72℃ for 45 secs.

Quantitative PCR (qPCR) targeting AmoA (ammonium-oxidizing archaea)-specific 16S rRNA gene sequence using the MCGI primers

For AmoA qPCR, the reaction mix consisted of 5x HOT FIREPol® EvaGreen® qPCR supermix, 0.2 µM Reverse (MCGI-554R) and Forward (MCGI-391F) primers (Table 1), Nuclease-free water, and the template DNA (eluted DNA from DNA extraction) which had a total volume of 20 µL. The following program was then used with the C1000 Touch™ Thermal Cycler (BioRad, USA): one cycle of 95℃ for 15 mins and 40 cycles of 95℃ for 30 secs, 60℃ for 30 secs, and 72℃ for 30 secs.

Table 1: List of forward and reverse primers used for product amplification in PCR and qPCR

Primers	Sequence (5'-3')	Target gene	Reference	Utilization
341F	CCTACGGGRBGCASCAG	Prokaryotic 16S rRNA	(Yu et al., 2005)	PCR and qPCR
806R	GGACTACYVGGGTATCTAAT	Prokaryotic 16S rRNA	(Yu et al., 2005)	PCR and qPCR
MCGI-391f	AAGGTTARTCCGAGTGRTTC	AmoA 16S rRNA	(De Corte et al., 2009)	qPCR
MCGI-554r	TGACCACTTGAGGTGCTG	AmoA 16S rRNA	(Teira et al., 2004)	qPCR

AmoA – ammonium-oxidizing archaea from the Thaumarchaeota phylum. F/f: forward, R/r: reverse.

2.4 Determination and quantification of cobalamin

2.4.1 Microbiological Assay

Preparation of Tryptic Soy Broth

A weight of 30 grams of Tryptic soy broth was added to a 1000 mL Duran glass bottle. Approximately 1000 mL MilliRo H_2O was then added and brought to a boil in a microwave oven to partially dissolve the powdered TSB. The solution was autoclaved at 121℃ for 15 minutes and then stored in a refrigerator at 1-4℃ until further use.

Preparation Tryptic Soy Agar

30 grams Tryptic Soy Broth and 15 grams of agar powder were mixed in a 1000 mL Duran glass bottle where approximately 1000 mL MilliRo H_2O was added. This was boiled in a microwave oven and then autoclaved at 121℃ for 15 minutes. The agar mixture was stored in a warm water bath at 55-60℃ to prevent solidification.

Preparation of the agar assay

Following the procedures described in Diding (1951), the following components were mixed in a 1000 mL Duran glass bottle: KH_2PO_4 (3 g), K_2HPO_4 (7 g), $MgSO_4*7H_2O$ (0.1 g), $C_6H_5Na_3O_7*2H_2O$ (0.5 g), $(NH_4)_2SO_4$ (1 g), agar powder (15 g), and ~990 mL MilliRo H_2O. The solution was then boiled in a microwave oven at was set for autoclaving at 121℃ for 15 minutes. A glucose stock was then added aseptically using a sterile 10 mL syringe (BD Plastipak™, Spain) and a 0.2 μm filter membrane (Sarsedt, Germany). The agar solution was stored in a warm bath at 55-60℃ until further use. Additionally, a minimal medium without agar, but with all the same components and measurements, was also created. This was used for diluting the overnight cultures of *E. coli* strains to obtain an optical density of 500 (OD_{500}).

Preparation of soft agar overlay

Using the same components, measurements, and methods as the agar assay, the soft agar overlay was prepared. For this particular technique however, less agar powder was used to create a less solid overlay (50% less). This was then stored in a warm bath at 55-60℃ until future use after the aseptical addition of glucose stock.

Cultivation of *Escherichia coli* strains

Two strains of *Escherichia coli* were cultivated for the present study: *E. coli* ATCC 11775 and *E. coli* ATCC 14169. The first strain was obtained from laboratory engineer, Else Marie Aasen, and the latter, was obtained from KwikStik MediMark© Europe (Microbiologics, France) and is a known cobalamin-dependent strain. Both strains were inoculated on the prepared plates containing solidified Tryptic Soy Agar using a sterile loop and incubated for 24 hours at 37℃. The plates containing strain colonies were stored at 4℃ until further use.

2.4.2 Enzyme-linked immunosorbent assay (ELISA)

Preparation of sediment samples

Approximately 250 µL of sediment sample were transferred to sterile 5 mL Eppendorf tubes and was mixed with 2 mL sample diluent (PBS buffer ready-to-use). Each tube was vortexed for 30 seconds. Then, Fastprep tubes were prepared by transferring beads of the following sizes into the tubes: 106 µm, 200-300 µm, and 2 mm. The sediment samples were then transferred to the tubes and were lysed using the MagNA Lyser (Roche Diagnostics, Germany) at 6200 rpm for 2x20 secs. After the lysing process, pH was measured using pH strips and was ensured to be between 6-7. 1M NaOH was used for deprotonation if the pH is too low, and vice versa, 1M HCl for a pH higher than the preferred range.

Enzyme Immunoassay for the Quantitative Determination of Vitamin B_{12} in Food protocol

The kit SENSI*Spec* ELISA Vitamin B_{12} 96 Tests (Eurofins Technologies, Hungary) and the protocol provided by the manufacturer was used for the ELISA. First, 50 µL of the supernatant generated from the sample preparation was aliquoted to the wells of a microtiter plate coated with anti-vitamin B_{12}. Immediately after, 50 µL conjugate vitamin B_{12}-peroxidase was added into each well. The microtiter plate was then covered with a plastic foil and was, with a shaking program, incubated in the VarioSkanLUX (Thermo Fisher Scientific, USA) for 60 minutes at about 22℃. Then, a series of washing steps were performed using a washing solution containing PBS and Tween 20. Next, substrate solution containing TMB (3,3',5,5-Tetramethylbenzidine), which is a chromogen, was added to each well resulting in a blue color after incubation in the dark for 20 minutes. A stop enzyme solution (0.5M H_2SO_4) was then added to stop the previous reaction. Upon addition, the blue color will turn into yellow. Lastly, the plate was gently mixed by shaking and absorbance at 450 nm (reference wavelength: 620 nm) was measured using the VarioSkanLUX plate reader (Thermo Fisher Scientific, USA).

2.5 Optimized protocol for parallel experimentation of ELISA and microbiological assay

First, approximately 150 µL of the sediment samples obtained from the microcosm pollution experiment were transferred in new Sarsedt containers and were autoclaved at 121℃ for 15 minutes based on the report that cobalamin could be bound to sediment particles (Nishijima & Hata, 1986) and the protocol for cobalamin extraction provided by Kumudha et al. (2010). Then, the samples were transferred to 5 mL Eppendorf tubes and were mixed with PBS buffer before vortexing for 30 seconds. The lysing step was skipped. The pH was afterwards measured using pH strips, in which the preferred range lie from 6 to 7. After pH measurement, the protocol provided by Eurofins for the ELISA was performed.

The remaining supernatant from the vortexed samples were then used for the microbiological assay as adapted from da Silva et al. (2021). First, prepared overnight cultures of both *E. coli* ATCC 14169 and 11775, were made beforehand by adding 10 mL Typtic Soy Broth to sterile glass tubes and mixing it with a single colony picked from premade pure cultures of both strains and were incubated at 37℃ for 24 hours with shaking. 1 mL of overnight cultures were transferred in 1.5 mL Eppendorf tubes and were centrifuged at 13000 rpm for 5 minutes at 22℃. The supernatants were discarded, and the obtained cell pellets were resuspended in 500 µL of 0.9% sterile NaCl. Then, the tubes were centrifuged, and the supernatants were discarded again. 1 mL of the minimal assay medium was then added to the tubes to resuspend the cell pellets. The resuspended supernatant was then transferred to new sterile test tubes each. Using the McFarland densitometer (BioSan Ltd., USA) to measure the OD of the supernatants were diluted with the minimal assay medium until approximately OD_{500} was achieved. Afterwards, 1 mL of the diluted supernatant was transferred to a sterile falcon tube which was then homogenized with the prepared 9 mL soft agar medium, having a ratio of 1:10. The contents of the tube were mixed vigorously through manual shaking, and were immediately poured over the surface of prepared agar plates. The plates were then air-dried for 30 minutes, and sterile paper discs were placed over the soft agar surface after. Sterile paper discs were picked using a sterile syringe with a needle, and another needle was used to carefully remove the disc from the syringe onto the surface of the soft agar overlay. Additional 5 minutes of air-drying was performed to prevent liquid dispersion, and the plates were finally incubated at 37℃ for 24 hours after putting the agar plates in a sterile plastic bag.

2.6 Statistical analysis

2.6.1 Data processing of 16S rRNA Illumina sequencing data

The data processing of the sequencing data was performed by Chief Engineer, Inga Leena Angell, and used the open-source tool VSEARCH in R (Rognes et al., 2016). Firstly, the reads from the sequencing data were trimmed to remove the first ten bases on the 3' end, then the reads were merged. After removing undesired primer sequences, quality filtering was performed to remove suboptimal sequences. Unique sequences were then allocated, in which sequences that had less than two copies were removed, while sequences that had multiple copies were kept. Then, Operational Taxonomic Unit (OTU), which are 16S rRNA sequences that share a certain percentage of similarity (Spohn & Young, 2018), clustering was performed to cluster sequences that had 97% or above in sequence similarity. Next was detecting and removing chimeras. Subsequently, an OTU table illustrating the number of total copies of each OTU within each sample was generated. The Phyloseq software package in R was then used to generate plots representing the post-clustering data (Figures 10-14) (McMurdie & Holmes, 2013).

2.6.2 Measurement of alpha (α) and beta (β) diversity

The α-diversity measures the ecological structure of a local community (Willis, 2019). In the present study, the metric that was used was taxonomic richness, as in the total number of observed OTUs within the samples taken from the enrichment media. As for the β-diversity, which is the measurement of dissimilarity of communities between different environments (Andermann et al., 2022), a Principal coordinates analysis (PCoA) plot based on Bray-Curtis dissimilarity metrics was generated. In PCoA, the percentage of variance between samples is represented and was used to visualize the proximity between each sample. The Bray-Curtis dissimilarity metrics measures the abundance of the same taxa or, in the present case, OTUs between all pairs of samples, and ranges from scores of 0 to 1, in which 0 represents a 100% shared relative abundance, while 1 represents 0% shared abundance (Kers & Saccenti, 2021).

3 Results

3.1 Optimization phase for methods used in determining cobalamin

3.1.1 Optimization of Enzyme-linked immunosorbent (ELISA) assay for cobalamin detection

The first optimization phase of ELISA was to test the effect of autoclaving on cobalamin release from sediment particles as described by Kumudha et al. (2010). This was performed using cobalamin-spiked sediment samples retrieved from Emmerstad Bay in Vestby municipality. At 10 ng/mL, absorbance results obtained from the autoclaved and non-autoclaved cobalamin-spiked sediments were as follows: 0.36 and 0.8, respectively. This indicated that that autoclaving might have enhanced the cobalamin dissociation from the sediments, since the concentration of cobalamin is inversely proportional to the absorbance measurement. Figure 2 illustrates a separate experiment that shows a retest of the autoclaving combined with the second optimization phase, which encompassed the test of impact when omitting the mechanical lysing step during the ELISA sediment sample preparation. As seen from Figure 2, the absorbance measurements obtained with mechanical lysis are higher at 1000, 100, and 10 ng/mL than the absorbance measurements when mechanical lysis was omitted. In essence, the samples that were not lysed indicated higher concentrations of cobalamin than the samples that were subjected to mechanical lysis during the sample preparation. In addition, only at the 1000 ng/mL sample that was not mechanically lysed where autoclaving displayed a slight advantage since the absorbance measurement was lower than its counterpart (Figure 2). The other samples showed that omitting autoclaving resulted in lower absorbance measurements with or without mechanical lysis. However, due to the uncertainty of the autoclaving results, this was further tested in future procedures. Duplicates of cobalamin-spiked sediment samples were then tested to finalize the optimization phase of ELISA. As seen in Figure 3, autoclaving yielded lower cobalamin concentrations since the average absorbance measurements were higher at all concentrations than the sediment samples that were not autoclaved. The lysing step was omitted during the finalization (Figure 3).

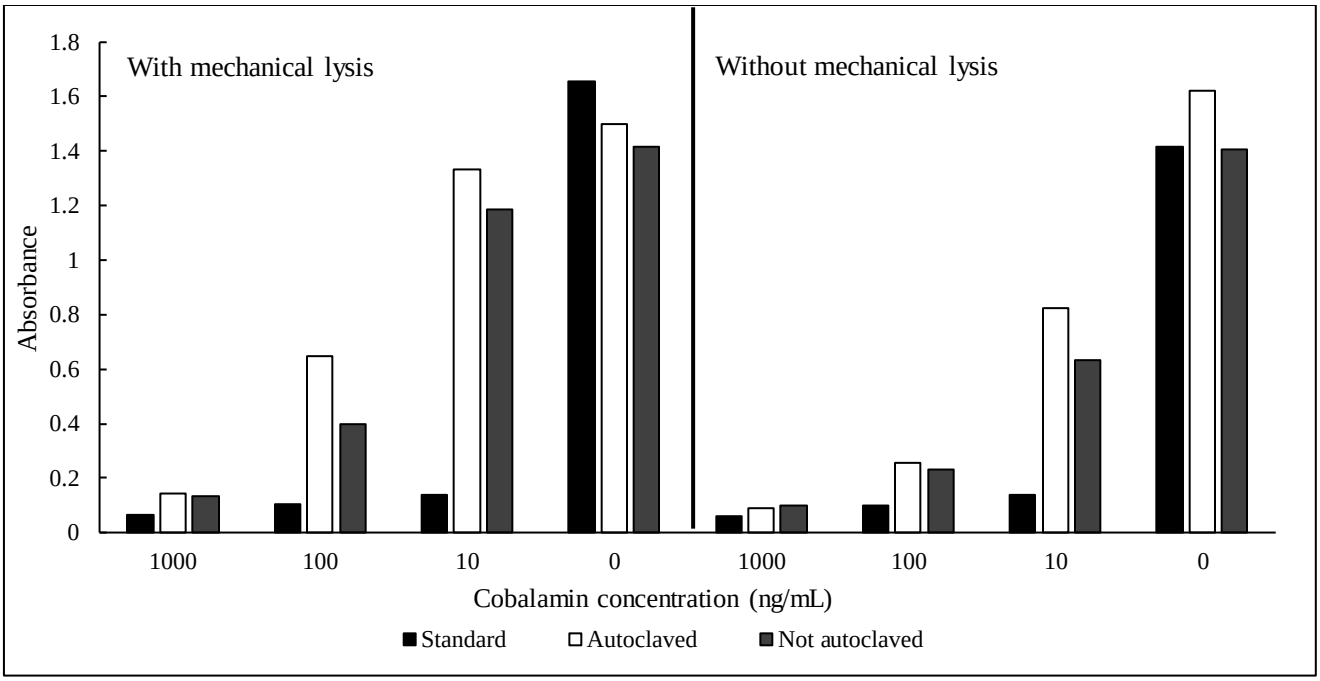

Figure 2: Comparison of differences in absorbance measurements at 450 nm. The difference between performing and omitting mechanical lysis during sample preparation as well as autoclaving and not autoclaving is indicated in the bar chart**.** Graph illustration of absorbance measurements after ELISA showing that cobalamin concentration is higher when the lysing procedure for ELISA was disregarded.

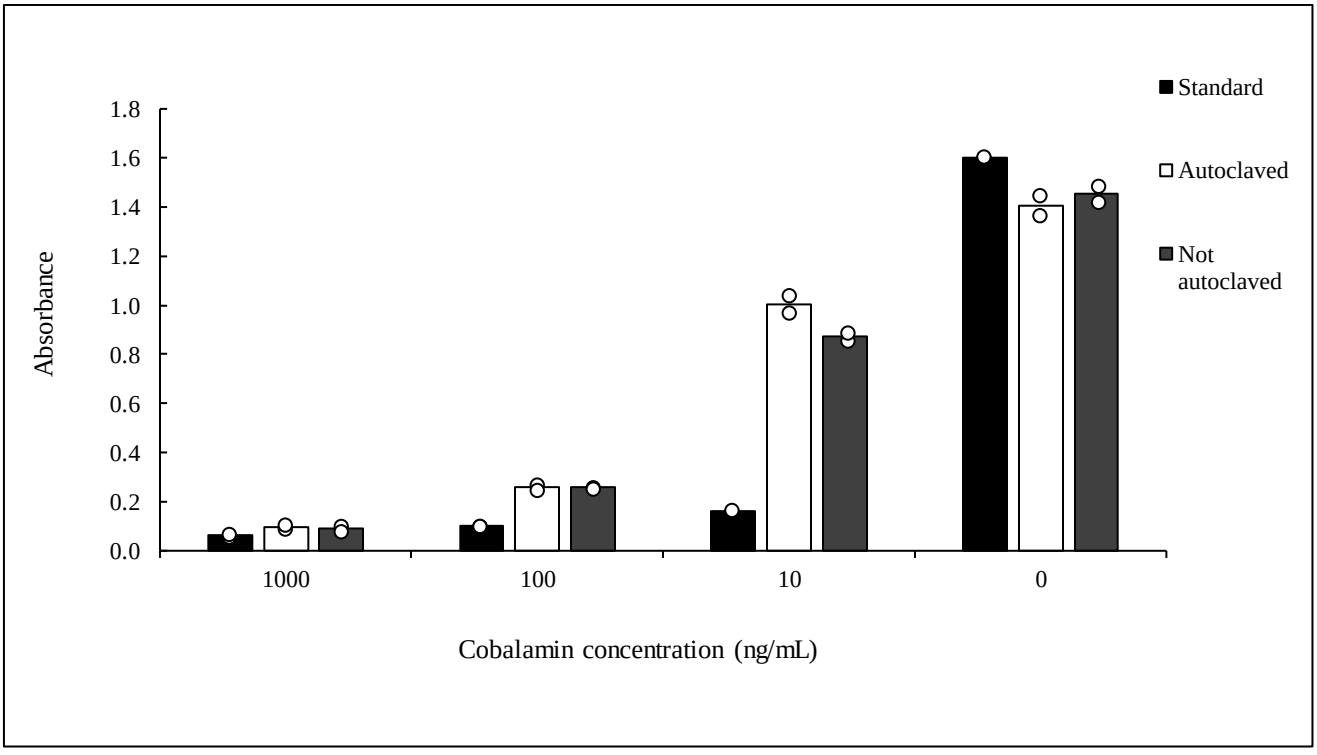

Figure 3: Illustration of absorbance measurements at 450 nm when mechanical lysis was omitted. Average values of duplicates for the standard, autoclaved, and not autoclaved cobalamin-spiked sediment samples were measured and are represented in the bar chart**.** The white transparent dots represent the individual data points in which the average was calculated from.

3.1.2 Optimization of microbiological assay for cobalamin detection

The microbiological assay was optimized based upon the protocol developed during the optimization phase of ELISA. Therefore, both autoclaving and omitting the lysing step were also tested during the optimization of the microbiological assay. The samples that were used in Figures 2 and 3 were also the samples that were utilized in both Figures 4 and 5, respectively. As seen in Figure 4, the zone diameters obtained from 1000 and 100 ng/mL when mechanical lysis was omitted, were, in average, larger compared to when the mechanical lysis was performed. Furthermore, at 10 ng/mL, it was observable that no growth zone was obtained when mechanical lysis was carried out. The zone diameters are illustrated in Supplementary material S.3.1-S.3.2. Duplicates of cobalamin-spiked sediment samples were then tested to finalize the optimization phase of microbiological assay as seen in Figure 5. There were small differences between the sediment samples that were autoclaved and those that were not (Figure 5).

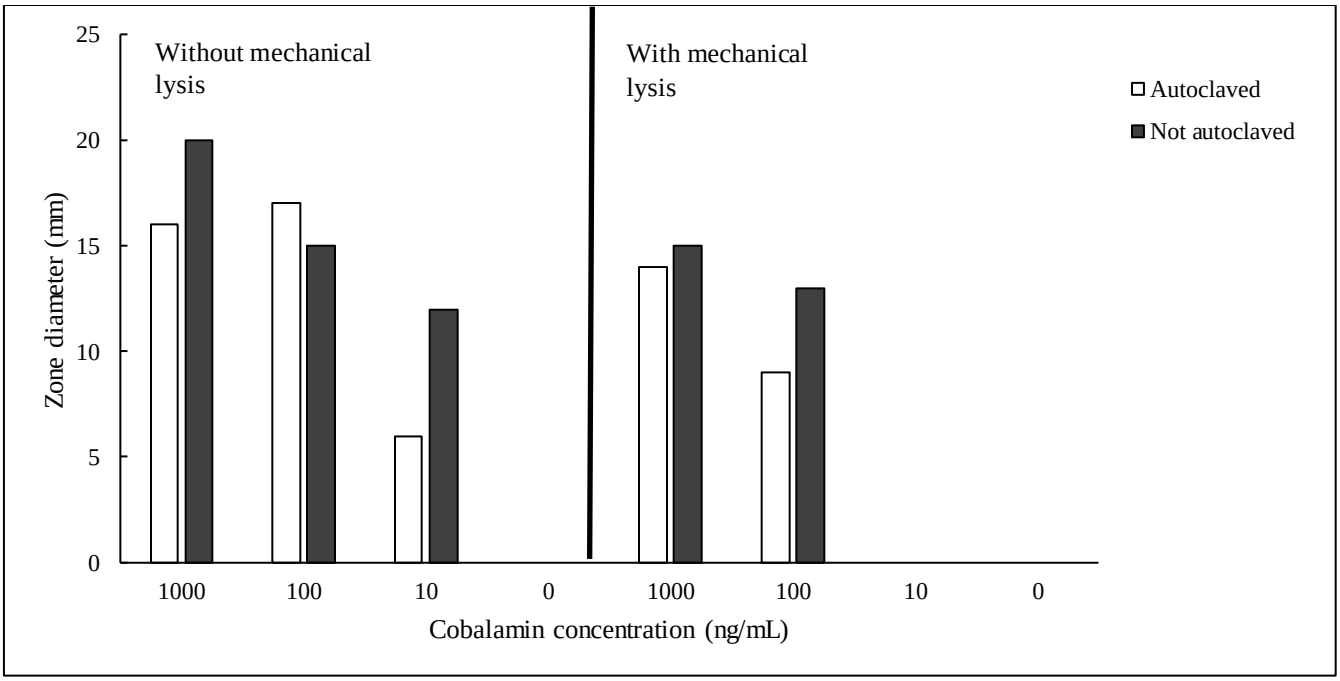

Figure 4: **Comparison of difference in zone diameters (mm).** The difference between performing and omitting mechanical lysis during sample preparation as well as autoclaving and not autoclaving is indicated in the bar chart. Cobalamin standards are missing.

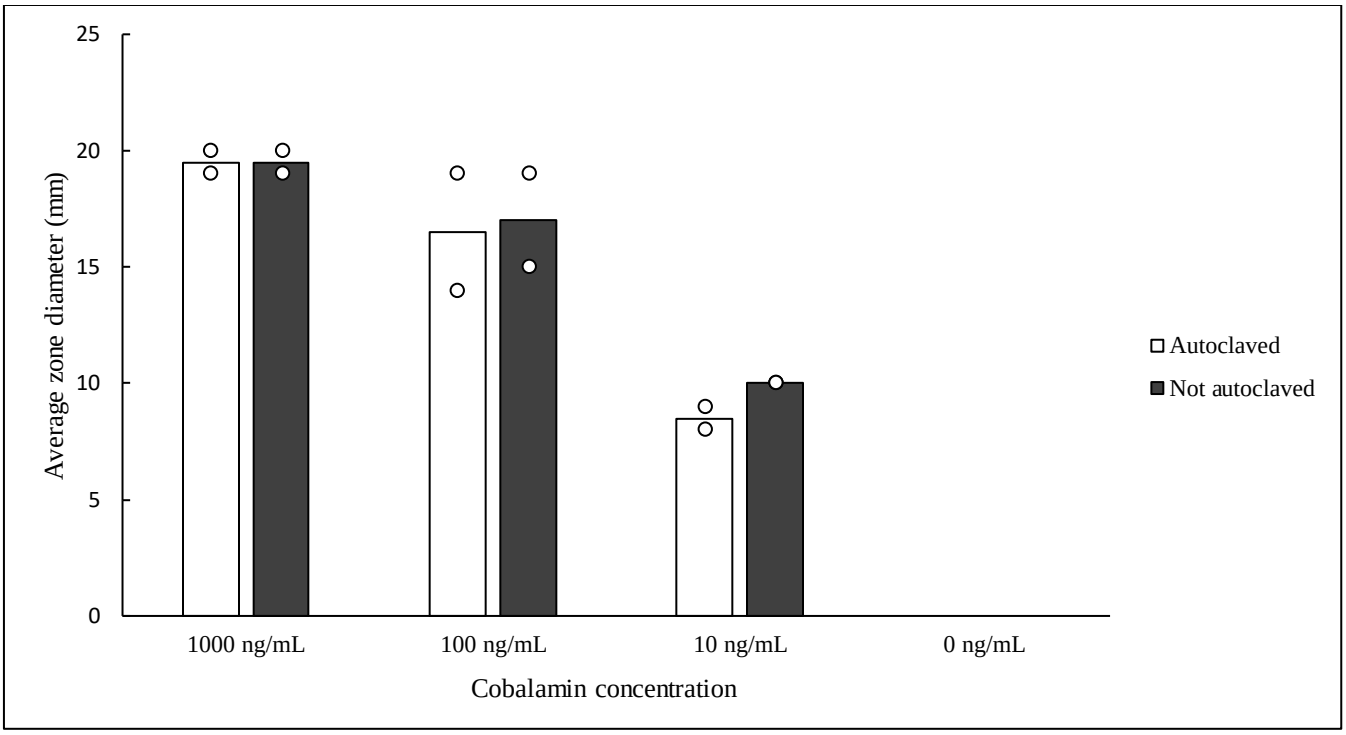

Figure 5: Illustration of average zone diameter (mm) when mechanical lysis was omitted. The duplicate average values for the standard, autoclaved, and not autoclaved cobalamin-spiked sediment samples were calculated and is indicated in the bar chart. The white transparent dots represent the individual data points in which the average was calculated from. Cobalamin standards are missing.

3.2 Determination and measurement of cobalamin using the optimized ELISA protocol

The initial samples (T0) from Hvitsten bay (n=3) and the extra T8 enriched sediment samples (n=18) were used to detect and measure cobalamin. The anoxic nitrate-reducing medium had the lowest absorbance measurement in average, indicating that it is the medium in which the highest concentration of cobalamin was detected. This was followed by the anoxic sulfate-reducing and the oxic sulfate-reducing media. The medium in which the lowest amount of cobalamin was detected was at the anoxic ammonium-oxidizing medium followed by the oxic ammonium-oxidizing medium as seen in Figure 6 and Supplementary material S.3.3.

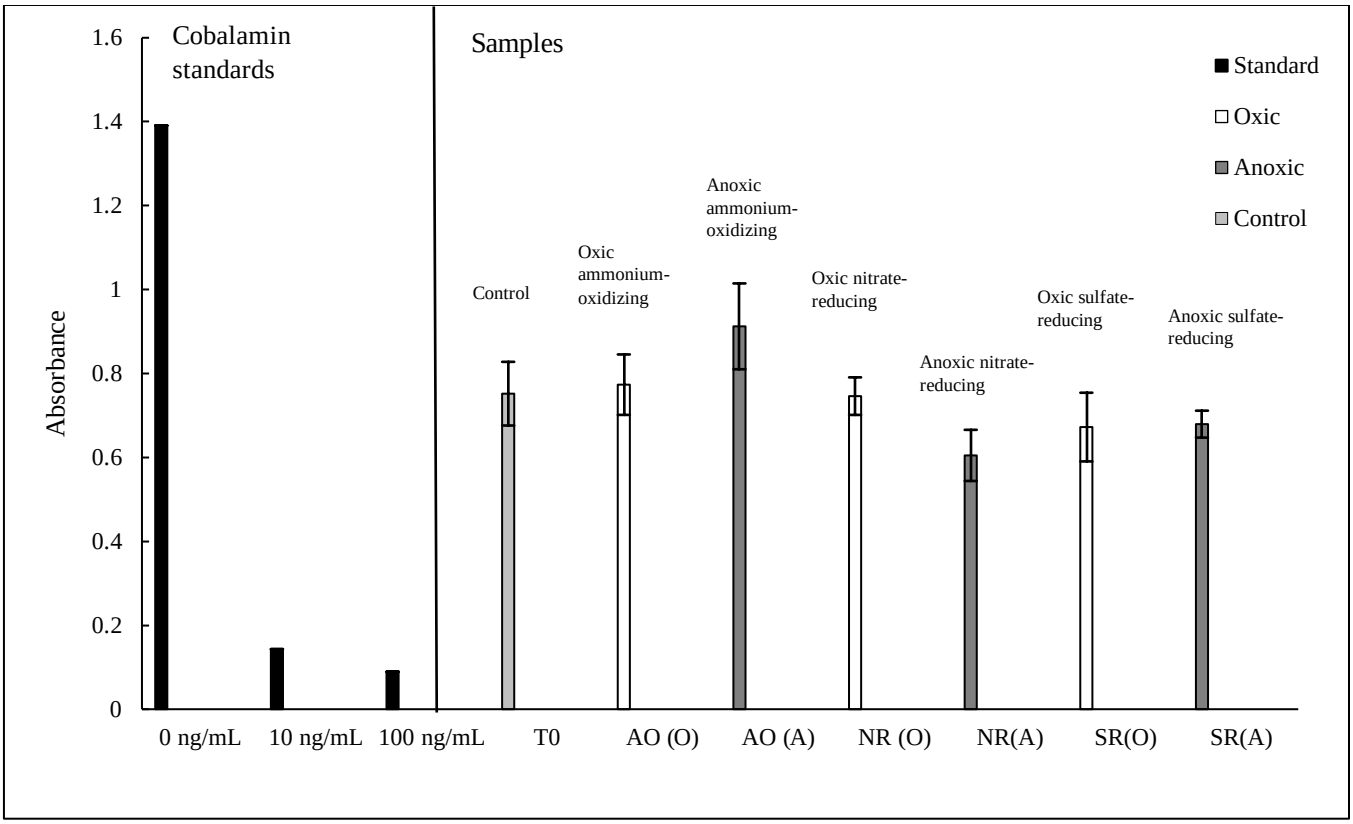

Figure 6: Representation of average absorbance measurements at 450 nm using triplicate samples from the enrichment media. The bar chart represents the average absorbance obtained from the standards, control, and the enrichment media**.** The legends represented by specific acronyms in the x-axis stand for the following: AO = ammonium oxidizing medium, NR = nitrate-reducing medium, and SR = sulfate-reducing medium. (A) = Anoxic and (O) = Oxic. All samples were autoclaved. The error bars represent standard deviations based on three data points.

3.3 Determination and measurement of cobalamin using the optimized microbiological assay protocol

The initial samples (T0) from Hvitsten bay (n=3) and the extra T8 enriched sediment samples (n=18) were used to detect and measure cobalamin. The average zone diameters obtained from the microbiological assay displayed a similar trend as the absorbance measurements from ELISA. As shown in Figure 7, the medium that generated the highest average zone diameter was the anoxic nitrate-reducing medium, followed by the anoxic and oxic sulfate-reducing media, respectively. The smallest average zone diameters were obtained from the oxic and anoxic ammonium-oxidizing media, similar to the ELISA results.

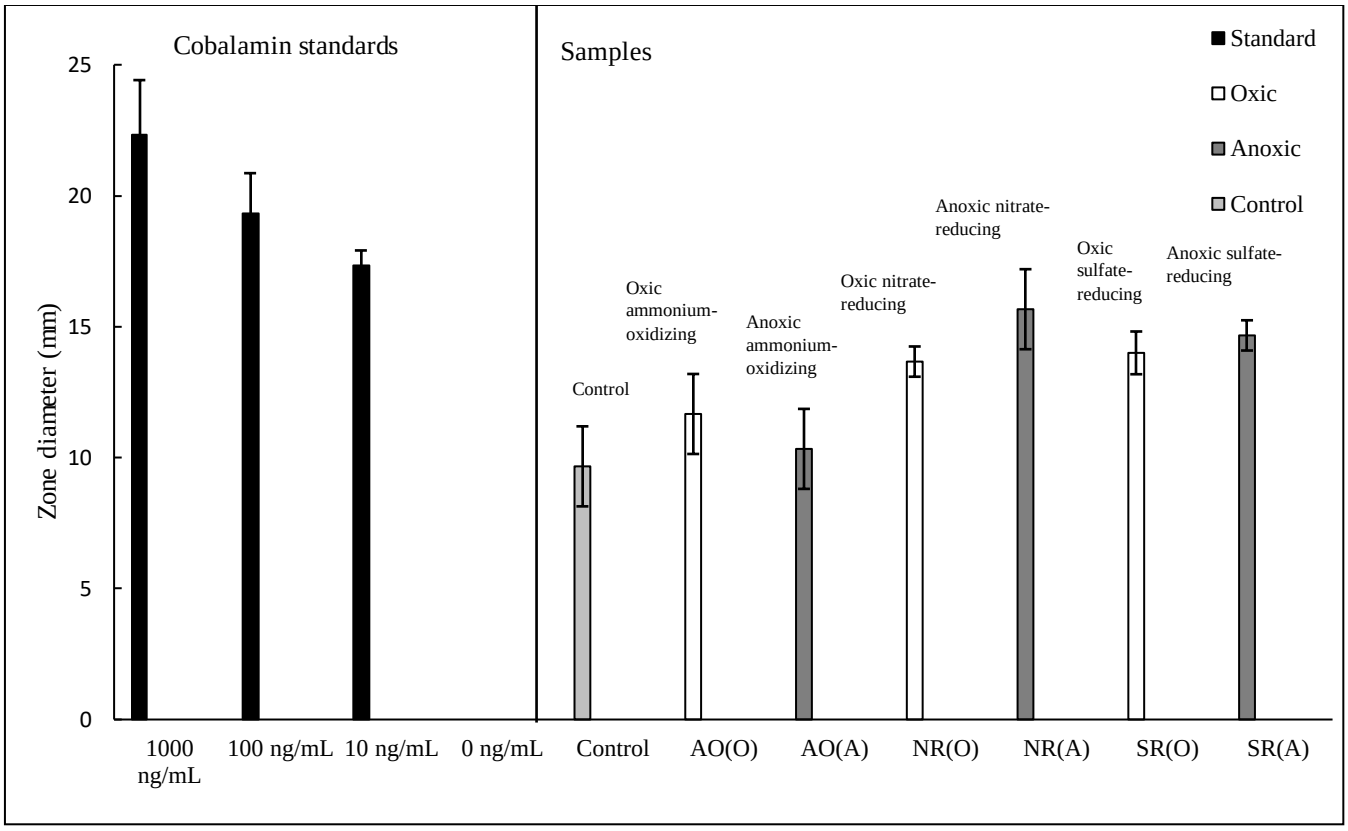

Figure 7: Representation of average zone diameter (mm) using triplicate samples from the enrichment media The bar chart represents the average zone diameter (mm) obtained from the standards, control, and the enrichment media**.** The legends represented by specific acronyms in the x-axis stand for the following: AO = ammonium oxidizing medium, NR = nitrate-reducing medium, and SR = sulfate-reducing medium. (A) = Anoxic and (O) = Oxic. All samples were autoclaved. All samples were autoclaved. The error bars represent standard deviations based on three data points.

3.4 Quantification cycle (C_q) values from Quantitative PCR

3.4.1 Universal prokaryotic primers targeting the 16S rRNA gene's V3-V4 region

Quantitative PCR (qPCR) was performed to detect and quantify the cell density in the samples from the microcosm pollution experiment. From the qPCR data, average C_q values from triplicates of every sample uptake from each medium were extracted. Overall, the values ranged from 15.9 to 28.0. High cell density was detected in each sample since the average C_q values in every single one was relatively low, except for the samples taken from the anoxic sulfate-reducing medium at T3 (Figure 8). This was the highest compared to the average C_q from the other media, thus a relatively low cell density. The lowest average C_q values were obtained from

the nitrate-reducing media in both conditions at T6 and T7. In addition, the average C_q values were lower at T1 than T8 for all media (Figure 8).

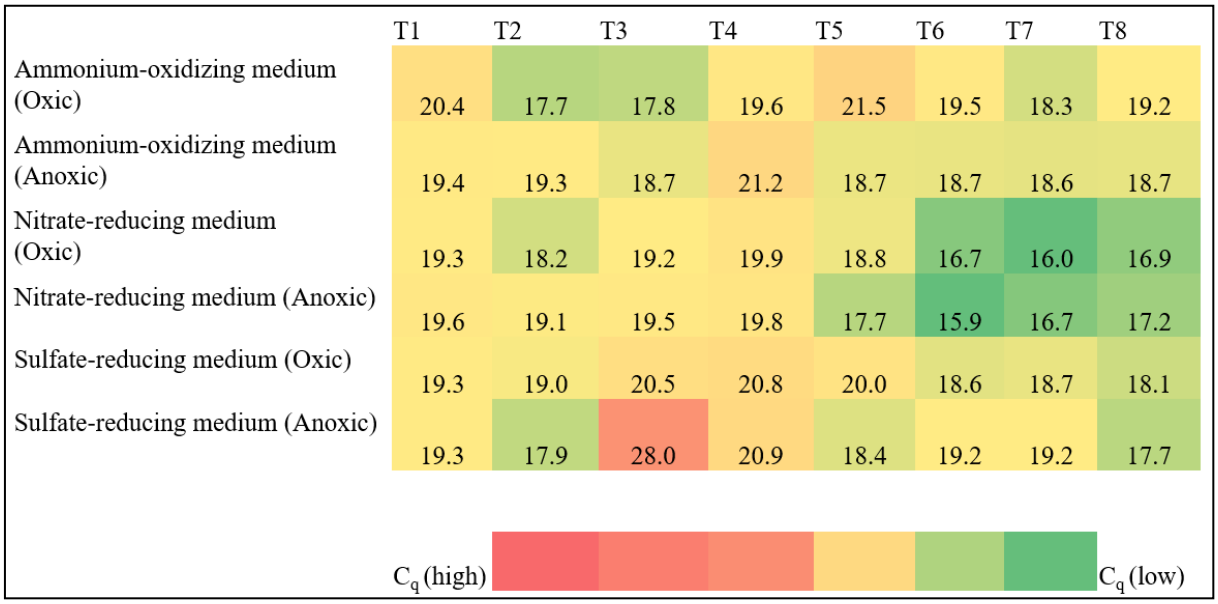

Figure 8: Heat map representing the average C_q values obtained from qPCR using universal prokaryotic primers targeting the 16S rRNA gene's V3-V4 region. The x-axis represents all the sample uptakes over the course of 4 weeks from T1 to T8. Media from which the samples were taken from are showed in the y-axis. The colored scales illustrate the relative microbial abundance in each media. Shades of orange to red illustrate ranges of high average C_q values, while the colors yellow to green represent lower average C_q values.

3.4.2 MCGI primers targeting the 16S rRNA gene's V3-V4 regions specific for ammonium-oxidizing archaea from the *Thaumarchaeota* phylum

Quantitative PCR using MCGI primers displayed that there was little to no observable detection of ammonium-oxidizing archaea within the enrichment samples. All the average C_q values were high (>32). The lowest average C_q value was retrieved from nitrate-reducing medium in the oxic condition at T3, while the lowest was observed in both anoxic nitrate-reducing and oxic sulfate-reducing medium at T5 and T8, respectively. At T1, all average C_q values were higher than the corresponding averages displayed in T8 for all media (Figure 9).

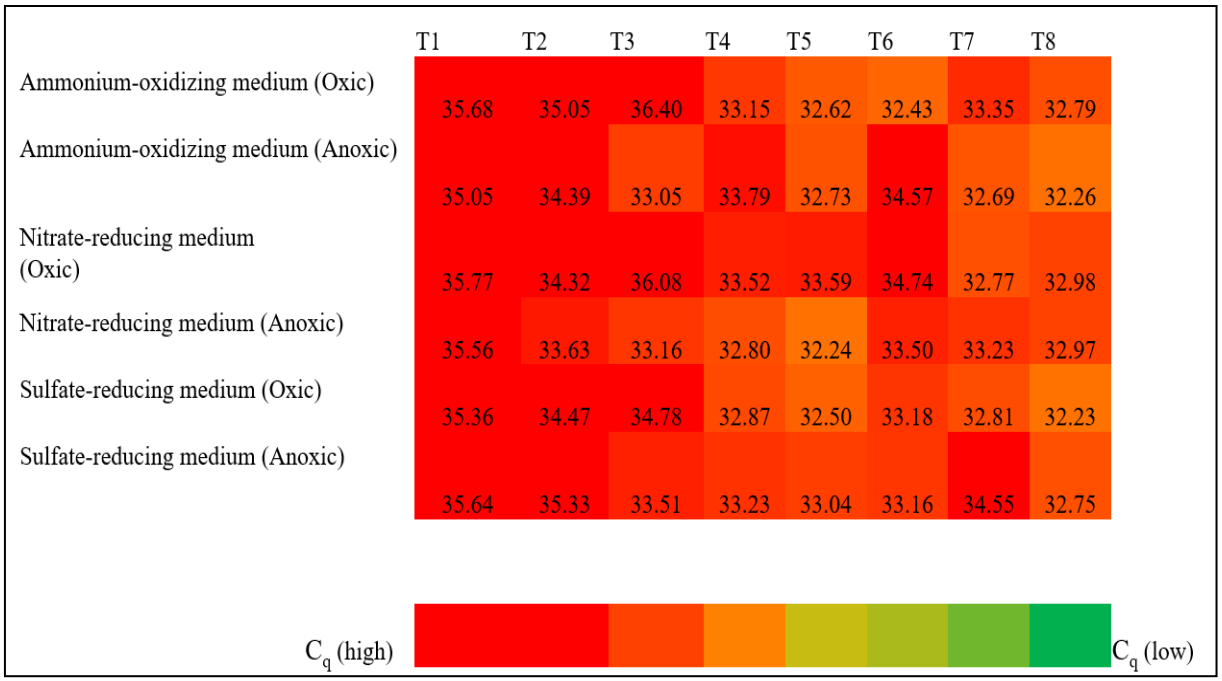

Figure 9: Heat map representing the average C_q values obtained from the qPCR using the MCGI primers targeting the 16S rRNA gene's V3-V4 regions specific for ammonium-oxidizing archaea from the *Thaumarchaeota* phylum. The x-axis represents all the sample uptakes over the course of 4 weeks from T1 to T8. The samples were taken from are indicated in the y-axis. The colored scales illustrate the relative microbial abundance in each media. Shades of orange to red illustrate ranges of high average C_q values, while the colors yellow to green represent lower average C_q values.

3.5 Determination of microbial composition and diversity via 16S rRNA gene sequencing

3.5.1 Comparison of phylum composition between two oxygen conditions

The phylum composition for the ammonium-oxidizing, nitrate-reducing, and sulfate-reducing media at both oxic and anoxic conditions was investigated using the sequencing data and Phyloseq software package in R studio. It was indicated that the set oxygen conditions amounted to little effects on overall phylum composition and abundance (Figure 10). All media were, to a large extent, composed of similar phyla of the following: *Proteobacteria*, *Cyanobacteria*, *Bacteroidetes*, *Actinobacteria*, and *Acidobacteria*. Additionally, all media, at both oxic and anoxic, the *Proteobacteria* phylum accounted for large proportions. The media in which the phylum displayed the most dominance is at both ammonium-oxiding media at approximately 55% of the phylum composition, and least at both nitrate-reducing media at roughly 40%. High abundance of the phylum *Campylobacterota* was observed in the nitrate-

reducing media, as well as the *Fusobacteria* phylum. In the sulfate-reducing media, the most abundant phylum, apart from *Proteobacteria*, was *Firmicutes* which accounted for approximately 20% of all phyla present within both media.

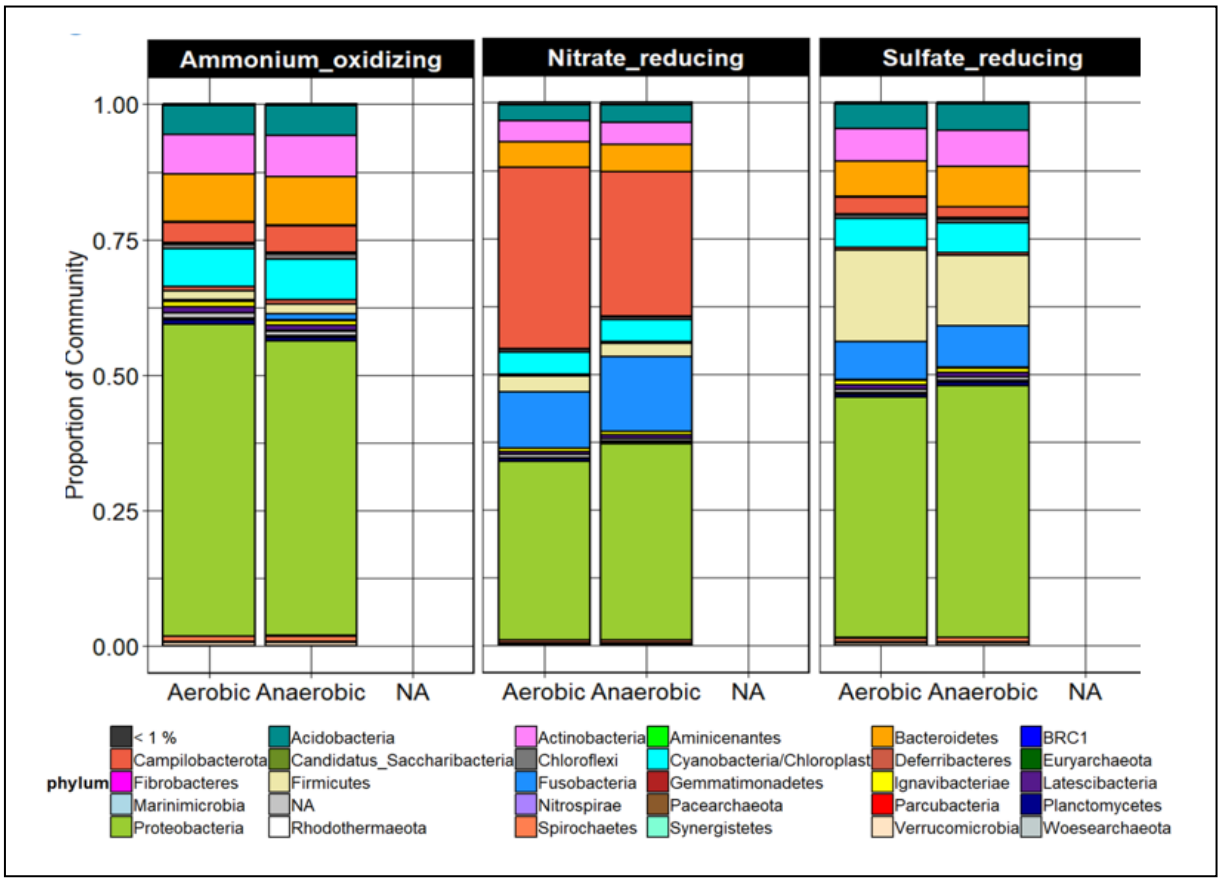

Figure 10: Comparison of phylum composition between sample uptakes from the enrichment media. The Phyloseq software package in R was used to generate the bar chart representing the most abundant phyla in the ammonium-oxidizing, nitrate-reducing, and sulfate-reducing media. The percentage of proportion (i.e., 1.00 = 100%) is indicated in the y-axis, while the sample uptakes and media in which the samples were retrieved from is represented by the x-axis. This chart was created by engineer, Inga Leena Angell.

3.5.2 Phylum composition of the sample uptakes

Using the sequencing data and the Phyloseq software package, the phylum composition from each sample uptake (T1-T8) from all media was also considered. Congruent to the results from the oxygen condition comparison, all the media consisted of mostly similar phyla (i.e., *Proteobacteria*, *Cyanobacteria*, *Bacteroidetes*, *Actinobacteria*, and *Acidobacteria*). The ammonium-oxidizing media consisted of similar phyla and were at consistent levels from T1-

T8. *Proteobacteria* accounted for more than 50% of all sample uptakes. In the nitrate-reducing media, the *Campylobacterota* phylum was detected in high proportions at T4-T8. At the same time, *Fusobacteria* started to emerge and increased in proportions from T2-T8. At T5-T6 the abundance of Firmicutes was nearly non-observable. Both *Firmicutes* and *Fusobacteria* became more observable in the sulfate-reducing media at T3. At T4, the proportions of *Firmicutes* became larger than the initial proportion at T1 (Figure 11).

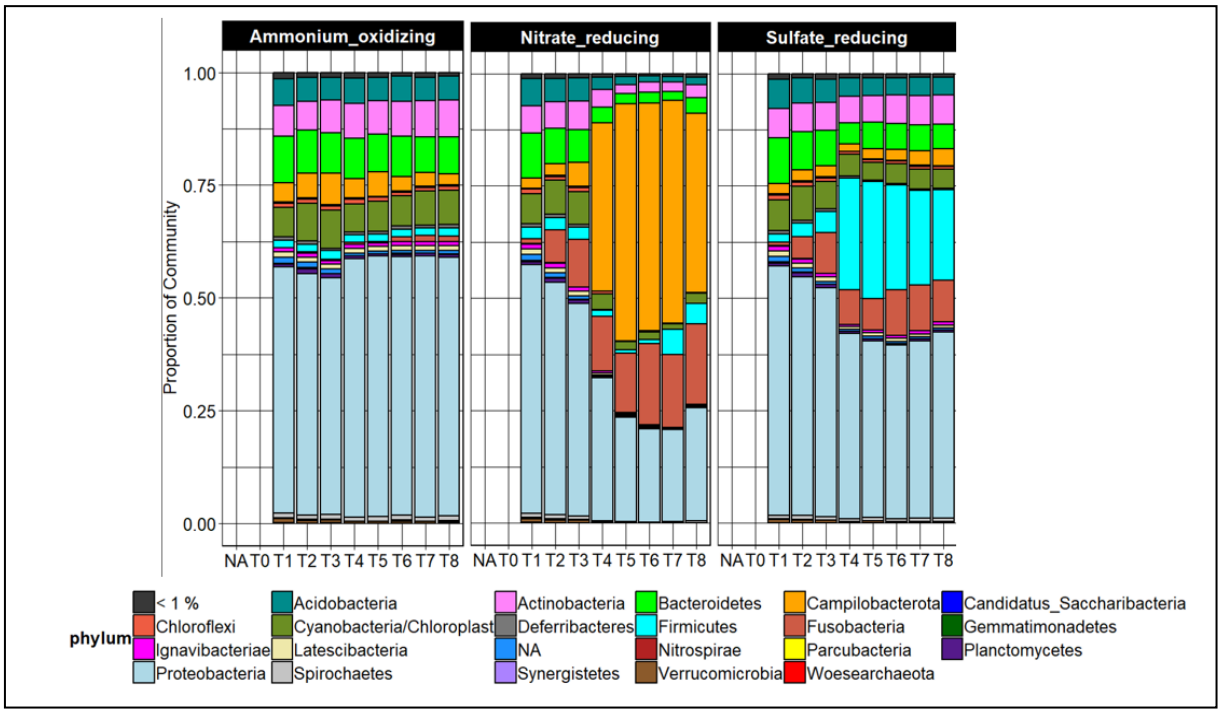

Figure 11: Comparison of phyla composition between sample uptakes from the enrichment media. The Phyloseq software package in R was used to generate the bar chart representing the most abundant phyla in the ammonium-oxidizing, nitrate-reducing, and sulfate-reducing media. The percentage of proportion (i.e., 1.00 = 100%) is indicated in the y-axis, while the sample uptakes in which the samples were retrieved from is represented by the x-axis. This chart was created by engineer, Inga Leena Angell.

3.5.3 Genus composition

To examine the microbial composition within the enrichment media more closely, the genus composition was also investigated. Firstly, in the ammonium-oxidizing media, most genera that were detected were present from T1-T8, each with a relatively similar proportion. The most abundant genera, in terms of proportions were *Bacillariophyta, Desulfosarcina,* and *Desulfatitalea*. In the nitrate-reducing media, the genera *Pseudoarcobacter*, *Arcobacter*, and *Propionigenium* accounted for high proportions of the total microbial abundance. This was

especially true for the genus *Pseudoarcobacter*, which started to dominate at T4. Lastly, the sulfate-reducing medium was dominated by the genus *Desulfonispora* which also started at T4 (Figure 12).

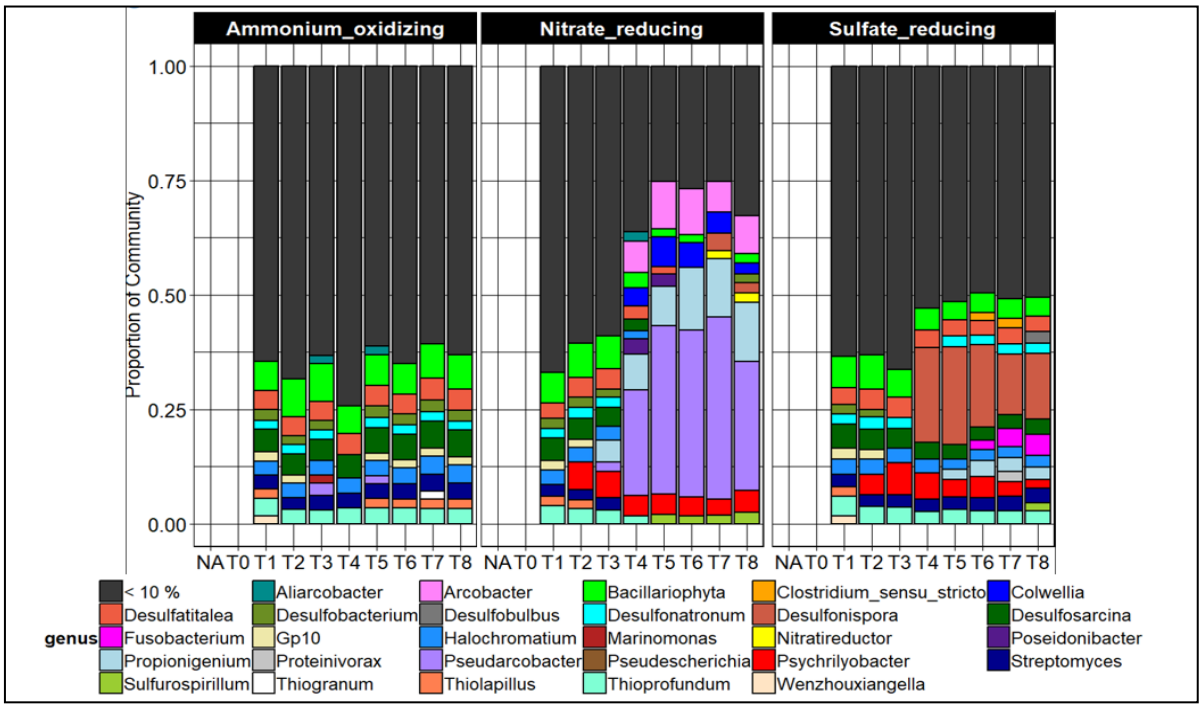

Figure 12: Comparison of genus composition between sample uptakes from the enrichment media. The Phyloseq software package in R was used to generate the bar chart representing the most abundant genera in the ammonium-oxidizing, nitrate-reducing, and sulfate-reducing media. The percentage of proportion (i.e., 1.00 = 100%) is indicated in the y-axis, while the sample uptakes in which the samples were retrieved from is represented by the x-axis. This chart was created by engineer, Inga Leena Angell.

3.5.4 Alpha (α) diversity

Using the sequencing data, the α-diversity within the ammonium-oxidizing, nitrate-reducing, and sulfate-reducing media at both oxic and anoxic conditions was investigated, in which richness, in terms of observed OTUs was the diversity metric of choice. The observed OTUs in the ammonium-oxidizing media were high at T1 but declined until T8. At T4, the media displayed its lowest number of observed OTUs. At T8, a slight increase in OTUs can be seen (Figure 13). In the nitrate-reducing media, the observed OTUs were relatively high as well. Like the former media, the number of observed OTUs dropped at T2-T3 and displayed a considerable drop at T4. The lowest total observed OTUs was at T7, which also had the lowest

range among all sample uptakes. OTUs increased faintly at T8. Lastly, high total observed OTUs was seen in the sulfate-reducing media at T1, and similar to the two other media, it began to decline at T2-T3. At T4, the total number of OTUs was relatively low and began to increase from T5-T8.

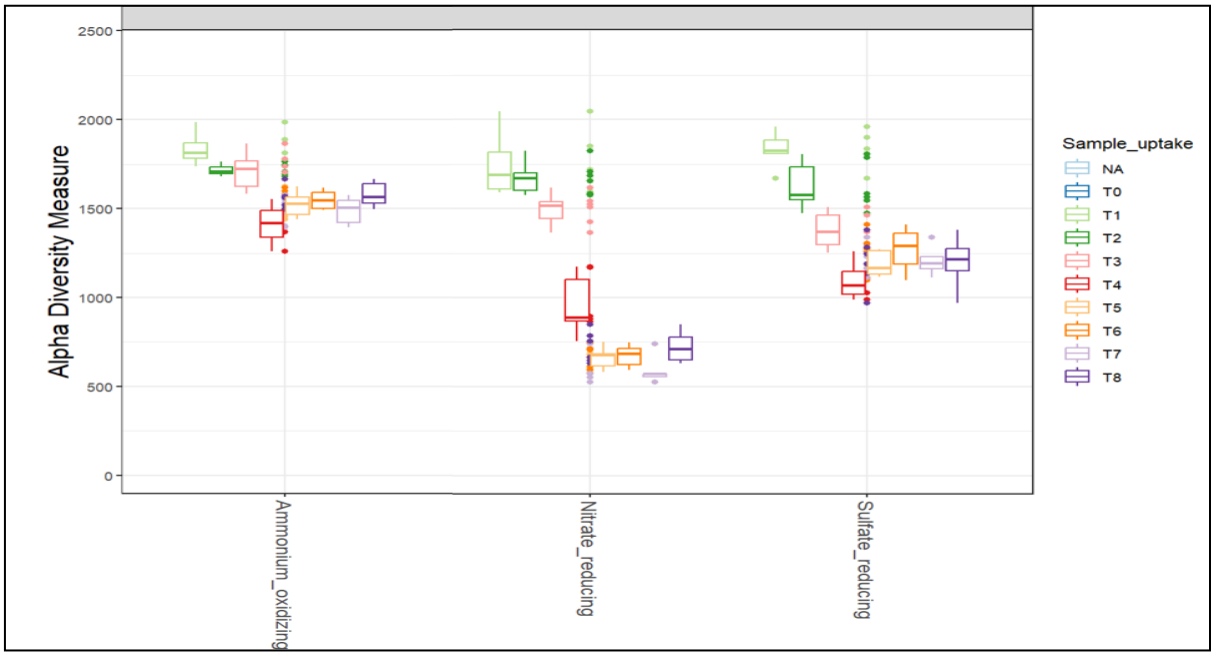

Figure 13: Measurement of observed OTUs within sample uptakes from the enrichment media. The Phyloseq software package in R was used to generate a measurement plot of the α-diversity or the species richness within the ammonium-oxidizing, nitrate-reducing, and sulfate-reducing media. The environments in which the samples were taken from are represented in the x-axis. Total number of observed species is indicated in the y-axis. This plot was created by engineer, Inga Leena Angell.

3.5.5 Beta (β) diversity

To compare the microbial diversity between the different enrichment media, the β-diversity was measured and was closely examined using the observed OTUs retrieved from the sequencing data. To a large extent, samples from all sample uptakes formed clusters. All samples from the ammonium-oxidizing media from T1-T8 were all clustered within coordinates around the top-left corner. The T1 samples of the nitrate-reducing media were closely clustered with the samples from the former but began to diverge at T2 and T3. The distance between T4 samples and the top-left cluster increased and continued to do so until T8 while forming a separate cluster around the top-right corner coordinates. The same observations were seen for the sulfate-

reducing media. T1 samples were clustered around the top-left corner and began to diverge from the immediate cluster at T2 and T3. Then, samples following and including T4 formed a separate cluster within the bottom-left corner. Furthermore, the percentage of variation between the samples from the ammonium-oxidizing and the sulfate-reducing media was lower than when the ammonium-oxidizing and the nitrate-reducing media was compared. The variance percentage was highest between T1 and T8 samples of the nitrate-reducing media. The composition dissimilarity score between the ammonium-oxidizing cluster or the initial cluster at T0 and the sulfate-reducing cluster was at about 0.25, while the overall composition dissimilarity score between the ammonium-oxidizing cluster or the initial cluster at T0 and the nitrate-reducing cluster was mostly between 0.4-0.6 (Figure 14).

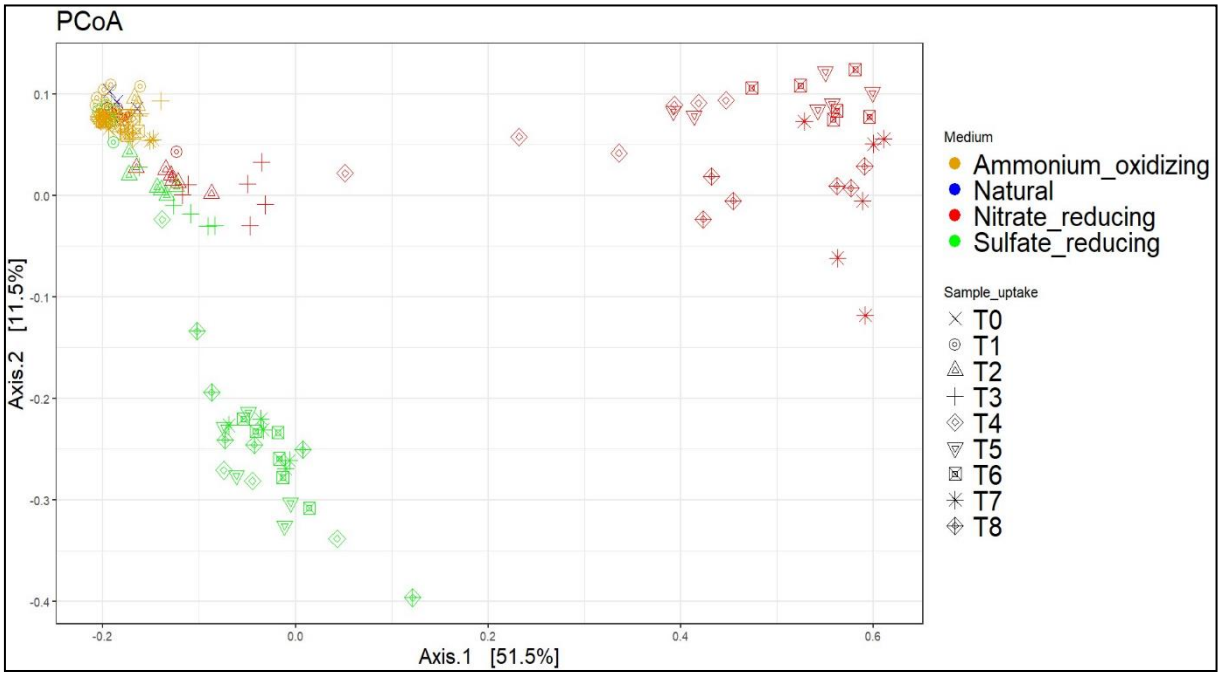

Figure 14: Comparison of OTU compositions from all sample uptakes within the enrichment media. The Phyloseq software package in the R was used to generate distances between the ammonium-oxidizing, nitrate-reducing, and sulfate-reducing media, then scatterplots were created using Principal Coordinates Analysis (PCoA) based on Bray-Curtis dissimilarity metrics. The index score is illustrated between samples taken from the different media as in a range between 0 and 1, where 0 represents the least dissimilarity and 1 as the most dissimilarity between two individual points. Axis 1. represents different factors that account for 51.5% of the variance between the samples and Axis 2 represents the further 11.5% variance. This plot was created by engineer, Inga Leena Angell.

4 Discussion

4.1 Microbial composition and diversity

Based on a key hypothesis by Pettersen et al. (2022) and a study conducted by Doxey et al. (2015), the initial expectation and a subgoal for the present study was to cultivate the ammonium-oxidizing archaeon *Nitrosopumilus* within an ammonium-oxidizing environment, but the results were not in line with the literature. Despite all the media consisting of most components necessary to cultivate *Nitrosopumilus*, they were underrepresented. Both qPCR data and the Phyloseq plots of phylum and genus composition showed indications of absence or underrepresentation of both *Thaumarchaeota* and *Nitrosopumilus* within the ammonium-oxidizing media, in both oxic and anoxic conditions. This observation was also the case for the nitrate- and sulfate-reducing media.

Furthermore, in terms of microbial composition and diversity, a plausible shift in the microbial composition may have occurred within the enriched media. This is based on the β-diversity measurement in Figure 14, as the initial cluster formation consisted of mostly sample uptakes from T1 in all media (Figure 14). The ammonium-oxidizing samples were all clustered from T1-T8 at a high extent. Samples from both the nitrate- and sulfate-reducing media, however, began to diverge from the cluster at around T2-T4 based on the variance percentage and the Bray-Curtis index scores. Consequently, both media formed two individual clusters with relative percentage of variance, in which the nitrate-reducing media displayed higher relative percentage of variance to the initial cluster than the sulfate-reducing media. In addition, the Bray-Curtis index score between the initial cluster at T1 and the cluster generated by the nitrate-reducing media was approximately 0.4-0.6. This could indicate medium to high compositional dissimilarity between the clusters. Similarly, the sulfate-reducing media also displayed this trend but with a lower Bray-Curtis index score between its cluster and the initial cluster at T1, which was mostly about 0.25. For the ammonium-oxidizing media, the dissimilarity from the initial cluster at T1 was relatively low, which ranged from 0 to 0.1, indicating that the composition was consistent from T1-T8 and a no to minimal change in compositional dissimilarity. Based on this knowledge, the compositional dissimilarity between the initial cluster formed at T1 by all media and the individual clusters formed by both nitrate- and sulfate-reducing media could be an indication of a compositional shift due to hypoxia and the addition of organic matter in both nitrate- and sulfate reducing media. Further, a low compositional

dissimilarity between the ammonium-oxidizing media cluster and the initial cluster at T1 was slightly expected because succinate was not added. This observation was consistent with Xu et al. (2022) describing the shift in organism composition caused by organic enrichment and hypoxia due to enhanced microbial metabolism in the benthic environment, and with Pettersen et al. (2022) which described the change in microbial composition in the benthic environments due to denitrification and/or sulfate-reduction reactions and organic enrichment. This could be explained by biogeochemistry shifts in the sediments due to excessive enrichment (Valdemarsen et al., 2012).

Moreover, in all media, the observed OTUs were all relatively high at T1. Based on the α-diversity measurement in Figure 13, the ammonium-oxidizing media displayed an OTU decline over time, but this could be explained by the fact that the plot combined both medium set at oxic and anoxic conditions, thereby also including the composition affected by the anoxic conditions. Nonetheless, the media displayed the relatively highest OTU richness among all enriched media. This was expected because succinate was not added to this medium, and is therefore, not organically enriched. In contrast, both organically enriched nitrate- and sulfate-reducing media displayed lower overall observed OTUs, especially the media where nitrate reduction reactions might have dominated. These observations were consistent with Pettersen et al. (2022), which described a correlation between denitrification to low OTU richness, and high OTU richness with ammonium-oxidizing environments. Moreover, excessive enrichment was also associated with the promotion of sulfate reduction, which can lead to accumulation of toxic gases (CH_4, H_2S), and thus might explain the low OTU diversity in the sulfate-reducing media (Valdemarsen et al., 2012). The findings in the present study may also be supported by Xu et al. (2022) as certain organisms in the present study may have been depleted on account of oxygen depletion caused by organic enrichment using succinate in both nitrate- and sulfate-reducing media and the anoxic parameters.

Additionally, the high degree of *Campylobacterota*'s sudden growth in the nitrate-reducing media at both oxic and anoxic conditions, might also be indicative of a microbial community shift due to hypoxia. This is because, the *Campylobacterota* phylum are obligate aerobes that cannot survive at oxygen concentrations above 10%, and might therefore thrive in hypoxic conditions (Skirrow, 2003). Moreover, in the nitrate-reducing media, detecting high proportions of the phylum *Fusobacteria*, which are generally obligately anaerobic, meant that anoxic conditions are environments they typically thrive in (Latta et al., 2015). The growth of these phylum in the media could be linked to previously mentioned conditions that could be linked

to microbial community shift within benthic environments, as these phyla were not detected initially at T1, and displayed sudden growth when the effects of the anaerobic chamber and succinate has taken place at T2-T8.

4.2 Cobalamin abundance in enrichment media

The abundance of cobalamin was initially expected to be highest in the ammonium-oxidizing media at oxic conditions, which was also based on the prediction from Pettersen et al. (2022) and the stated description about the ammonium-oxidizing archaea belonging to the *Thaumarchaeota* phylum as the most relevant cobalamin-producers in the marine environment by Doxey et al. (2015) and Law et al. (2021). However, based on the cobalamin determination assays, the preliminary expectation was not met in the present study. This was because, in ELISA, the highest absorbance measurements were detected in the anoxic ammonium-oxidizing media, followed by its oxic complement. This indicated that the lowest abundance of cobalamin was detected within the ammonium-oxidizing media. Unexpectedly, it was the anoxic nitrate-reducing medium that had the lowest absorbance measurement, which meant that cobalamin was most likely the highest in this medium. Further, both sulfate-reducing media and the oxic nitrate-reducing medium were among the media in which high cobalamin abundance was also detected in, but not higher than the anoxic nitrate-reducing medium (Figure 7). In addition, the results from the microbiological assay displayed a similar trend, in which the growth of a known cobalamin dependent *E. coli* ATCC 14169 was highest in the anoxic nitrate-reducing medium and lowest in the oxic ammonium-oxidizing medium, despite the initial expectation that the strain would thrive best in the latter.

Moreoever, observations from Doxey et al. (2015) suggests that aside from *Thaumarchaeota*, *Alpha-* and *Gammaproteobacteria, Bacteroidetes,* and *Cyanobacteria* are among the most relevant cobalamin producers in the marine environment. These are phyla that were detected in the ammonium-oxidizing media and displayed relatively high proportions in these media. Nonetheless, both nitrate- and sulfate-reducing media still displayed relatively higher concentrations of cobalamin than the ammonium-oxidizing media.

A possible explanation for the high concentrations of cobalamin in nitrate- and sulfate-reducing media could be the presence of pseudocobalamin instead of true cobalamin. ELISA might have detected pseudocobalamin instead of cobalamin, and this might have been the same compound that supported the growth of *E. coli* ATCC 14169 in unexpected environments. Cell density could also be a possibility for uncertainty in cobalamin concentrations within the media. This

is because, based on the qPCR results using universal primers, at T8, the nitrate-reducing media had the lowest average C_q values, followed by the sulfate-reducing media, then the ammonium-oxidizing media. This indicates that the nitrate-reducing media might have had the most cell density while the ammonium-oxidizing media had the lowest. The qPCR data could therefore be a parallel representation of the cobalamin measurements within all media.

Alternatively, the results from the cobalamin determination assays could be indicative of the presence of cobalamin producers that flourish or are able to survive in either hypoxic/anoxic, denitrifying, or sulfate-reducing environments. According to a study conducted by Piwowarek et al. (2018), several bacteria that belong to the genus *Propionigenium* have the genetic capacity to biosynthesize an active form of cobalamin. Interestingly, this genus was detected in both nitrate- and sulfate-reducing media, and plausibly, little detection of it within the ammonium-oxidizing media (Figure 12). Moreover, the detected proportions were higher in the nitrate-reducing media than the sulfate-reducing media, which were in line with the detected cobalamin abundance from both ELISA and microbiological assay. The relative proportions of detected *Propionigenium* could therefore be a plausible explanation for the cobalamin determination results in the present study.

4.3 Technical considerations for the assay optimizations

Autoclaving of sediments, which encompassed the first optimization phase of ELISA and microbiological assay to extract particle-bound cobalamin and was described in Kumudha et al. (2010), might not be an optimal method based on the results of the present study. It was observed that throughout the experiment, sediment samples that were not autoclaved yielded more desirable results, which was not congruent to the protocol provided by the literature (Kumudha et al., 2010). By the same token, mechanical lysis during the sediment sample preparation for ELISA unexpectedly yielded suboptimal results compared to when the step was omitted. Based on this knowledge, it might be more optimal to simplify the protocol, by for instance, omitting both the autoclaving and mechanical lysing of the sediments. This is strongly supported by the results from both ELISA and microbiological assay in Figures 2-5.

Furthermore, the addition of the seeded soft agar overlay on the surface of the more solid agar layer for the microbiological assay provided desirable results. Experimental agar assays preceding the addition of a soft agar overlay yielded no to little microbial growth on the hard agar surface. In contrast, with the overlay, visible growth zones were generated, and measurement of their diameters was finally possible. The softer and more fluid nature of the

soft agar overlay may be the reason for nutrients to plausibly become more available to the bacteria, hence its growth. Alternatively, pipetting cobalamin onto the surface of the agar may not be the best method to introduce it to the bacteria because the solution could have been subjected to evaporation and dispersion while incubation occurs. Perhaps, that is why seeding the bacteria into the soft agar overlay medium where nutrients could be easier to access may have favored their growth.

4.4 Limitations of the study and future perspectives

Although the present study did share similarities to a few observations from recent studies, there are still several limitations that ought to be mentioned. First, the cobalamin determination assays that were utilized in the present study were among the simplest of the possible alternative methods. By utilizing and/or adding on complex methods such as High-Performance Liquid Chromatography (HPLC) or Radioimmunoassay (RIA), uncertainties about the detection of either cobalamin or pseudocobalamin may have been avoided. Based on the results pertaining to the detection of cobalamin in unexpected environments, these more complex methods could provide further support to the methods that were utilized in the present study. Additionally, HPLC could also provide more rapid results and could be less labor intensive compared to both ELISA and microbiological assay. Limitations on microbiological assay were also present, as the author of the present study unintentionally excluded standards during the optimization phase. These were errors that may have affected the data analysis and may have contributed to the uncertainty of the cobalamin determination results. In addition, analytical approaches to determine compounds associated with excessively enriched sediments such as CH_4 and H_2S could be useful to further verify the effects of organic enrichment on the benthic ecosystem.

Furthermore, more sediment samples from the enrichment media could have been retrieved to gain more reliable and validating results, as in the present study, only triplicates from each medium were retrieved for each sample uptake. A larger sample size from each medium may be optimal for more valid results. In addition, for each sample uptake, the anaerobic chamber was opened and the media that was supposed to be set in anoxic conditions were exposed to oxygen for a brief period of time. There were also instances in which the anaerobic indicator detected oxygen in the chamber during incubation. These could have had potential effects on the microbial composition in all the anoxic media. For instance, the parallel growth of *Campylobacterota* as obligate aerobes and *Fusobacteria* as obligate anaerobes at T4 in the nitrate-reducing media at both oxic and anoxic conditions is enough to cause a doubt in the

contemporary oxygen parameters that were intended for the experiment. It could also be beneficial for future research, if possible, consider examining the composition at the species level. This could provide more specific insight into the roles of each microbial species and narrow down its' role in cobalamin production.

5 Conclusion

The present study was not able to enrich the ammonium-oxidizing archaeon, *Nitrosopumilus*, in the ammonium-oxidizing media, and was therefore not consistent with the hypothesis by Pettersen et al. (2022). In addition, the correlation between cobalamin and an ammonium-oxidizing environment that was predicted by Pettersen et al. (2022) was also not observed in the present study, because the lowest cobalamin concentrations were detected within the ammonium-oxidizing media, and highest within the nitrate-reducing media, followed by the sulfate-reducing media. Nonetheless, low OTU richness was observed in both nitrate- and sulfate-reducing media, while higher OTU richness was observed in the ammonium-oxidizing media. These results were parallel to a key observation by Pettersen et al. (2022). A shift in the sediment-associated microbial community within the enriched media might also have occurred based on both α- and β-diversity measurements and the Phyloseq plots containing the phylum and genus composition of all media. Furthermore, there might be a potential link between the high cobalamin concentrations in both nitrate- and sulfate-reducing media with the detection of the *Propionigenium* genus, which has the genetic capacity for cobalamin production. These findings, especially the implication of *Propionigenium* in the cobalamin reservoir in the marine benthic ecosystem should be examined closely for future research and verification. The optimization of cobalamin determination assays used in the present study also provided insight into how omitting some key procedures and using a soft agar overlay for the microbiological assay might have been beneficial during the optimization phase. Further research to verify the correlation between cobalamin abundance and OTU richness is recommended. In addition, the role of *Propionigenium* in cobalamin production within the marine benthic ecosystem ought to be included in future investigations.

Bibliography

Abu El-Regal, M. A., & Ibrahim, N. K. (2014). Role of mangroves as a nursery ground for juvenile reef fishes in the southern Egyptian Red Sea. *The Egyptian Journal of Aquatic Research*, *40*(1), 71-78. https://doi.org/https://doi.org/10.1016/j.ejar.2014.01.001

Ahmad, A., Sheikh Abdullah, S. R., Hasan, H. A., Othman, A. R., & Ismail, N. I. (2021). Aquaculture industry: Supply and demand, best practices, effluent and its current issues and treatment technology. *Journal of Environmental Management*, *287*, 112271. https://doi.org/https://doi.org/10.1016/j.jenvman.2021.112271

Alhajj, M., Zubair, M., & Farhana, A. (2023). Enzyme Linked Immunosorbent Assay. In *StatPearls [Internet]*. https://www.ncbi.nlm.nih.gov/books/NBK555922/

Alongi, D. M. (2020). Carbon Balance in Salt Marsh and Mangrove Ecosystems: A Global Synthesis. *Journal of Marine Science and Engineering*, *8*(10), 767. https://www.mdpi.com/2077-1312/8/10/767

Andermann, T., Antonelli, A., Barrett, R. L., & Silvestro, D. (2022). Estimating Alpha, Beta, and Gamma Diversity Through Deep Learning [Original Research]. *Frontiers in Plant Science*, *13*. https://doi.org/10.3389/fpls.2022.839407

Athanasopoulou, K., Boti, M. A., Adamopoulos, P. G., Skourou, P. C., & Scorilas, A. (2022). Third-Generation Sequencing: The Spearhead towards the Radical Transformation of Modern Genomics. *Life*, *12*(1), 30. https://www.mdpi.com/2075-1729/12/1/30

Balabanova, L., Averianova, L., Marchenok, M., Son, O., & Tekutyeva, L. (2021). Microbial and Genetic Resources for Cobalamin (Vitamin B12) Biosynthesis: From Ecosystems to Industrial Biotechnology. *International Journal of Molecular Sciences*, *22*(9), 4522. https://www.mdpi.com/1422-0067/22/9/4522

Barbier, E. (2017). Marine ecosystem services. *Current Biology*, *27*(11), R507-R510. https://doi.org/https://doi.org/10.1016/j.cub.2017.03.020

Bhatia, S., & Dahiya, R. (2015). Chapter 4 - Concepts and Techniques of Plant Tissue Culture Science. In S. Bhatia, K. Sharma, R. Dahiya, & T. Bera (Eds.), *Modern Applications of Plant Biotechnology in Pharmaceutical Sciences* (pp. 121-156). Academic Press. https://doi.org/https://doi.org/10.1016/B978-0-12-802221-4.00004-2

Bhavsar, R. B., Makley, L. N., & Tsonis, P. A. (2010). The other lives of ribosomal proteins. *Hum Genomics*, *4*(5), 327-344. https://doi.org/10.1186/1479-7364-4-5-327

Borges, A. V., & Abril, G. (2011). 5.04 - Carbon Dioxide and Methane Dynamics in Estuaries. In E. Wolanski & D. McLusky (Eds.), *Treatise on Estuarine and Coastal Science* (pp. 119-161). Academic Press. https://doi.org/https://doi.org/10.1016/B978-0-12-374711-2.00504-0

Bremner, J., Rogers, S. I., & Frid, C. L. J. (2003). Assessing functional diversity in marine benthic ecosystems: a comparison of approaches. *Marine Ecology Progress Series*, *254*, 11-25. https://www.int-res.com/abstracts/meps/v254/p11-25/

Butler, J. E. (2000). Enzyme-linked immunosorbent assay. *J Immunoassay*, *21*(2-3), 165-209. https://doi.org/10.1080/01971520009349533

Canene-Adams, K. (2013). Chapter Twenty Four - General PCR. In J. Lorsch (Ed.), *Methods in Enzymology* (Vol. 529, pp. 291-298). Academic Press. https://doi.org/https://doi.org/10.1016/B978-0-12-418687-3.00024-0

Chislock, M. F., Doster, E., Zitomer, R., & Wilson, A. E. (2013). Eutrophication: Causes, consequences, and controls in aquatic ecosystems. *Nature Education Knowledge*, *4*.

Claustre H., Legendre L., Boyd P. W., & M., L. (2021). The Oceans' Biological Carbon Pumps: Framework for a Research Observational Community Approach. *Frontiers in Marine Science*, *8*. https://doi.org/https://doi.org/10.3389/fmars.2021.780052

Covich, A. P., Austen, M. C., BÄRlocher, F., Chauvet, E., Cardinale, B. J., Biles, C. L., Inchausti, P., Dangles, O., Solan, M., Gessner, M. O., Statzner, B., & Moss, B. (2004). The Role of Biodiversity in the Functioning of Freshwater and Marine Benthic Ecosystems. *BioScience*, *54*(8), 767-775. https://doi.org/10.1641/0006-3568(2004)054[0767:Trobit]2.0.Co;2

da Silva, R. T., de Souza Grilo, M. M., Magnani, M., & de Souza Pedrosa, G. T. (2021). Double-Layer Plaque Assay Technique for Enumeration of Virus Surrogates. In M. Magnani (Ed.), *Detection and Enumeration of Bacteria, Yeast, Viruses, and Protozoan in Foods and Freshwater* (pp. 157-162). Springer US. https://doi.org/10.1007/978-1-0716-1932-2_14

Dang, H. (2020). Grand Challenges in Microbe-Driven Marine Carbon Cycling Research. *Frontiers in Microbiology*, *11*. https://doi.org/https://doi.org/10.3389/fmicb.2020.01039

Danovaro, R., Corinaldesi, C., Dell'Anno, A., & Rastelli, E. (2017). Potential impact of global climate change on benthic deep-sea microbes. *FEMS Microbiology Letters*, *364*(23). https://doi.org/10.1093/femsle/fnx214

De Corte, D., Yokokawa, T., Varela, M. M., Agogué, H., & Herndl, G. J. (2009). Spatial distribution of Bacteria and Archaea and amoA gene copy numbers throughout the water column of the Eastern Mediterranean Sea. *The ISME Journal*, *3*(2), 147-158. https://doi.org/10.1038/ismej.2008.94

De La Rocha, C. L., & Passow, U. (2014). The Biological Pump. In *Treaties on Geochemistry* (Vol. 8, pp. 93-122). Elsevier. https://doi.org/https://doi.org/10.1016/B978-0-08-095975-7.00604-5

Decho, A. W., & Gutierrez, T. (2017). Microbial Extracellular Polymeric Substances (EPSs) in Ocean Systems. *Front Microbiol*, *8*, 922. https://doi.org/10.3389/fmicb.2017.00922

Diding, N. (1951). A Simple Cup Assay of Vitamin B12 with a Stable B12-Requiring Mutant of Escherichia Coli. *Scandinavian Journal of Clinical and Laboratory Investigation*, *3*(3), 215-216. https://doi.org/10.3109/00365515109060602

Doxey, A. C., Kurtz, D. A., Lynch, M. D. J., Sauder, L. A., & Neufeld, J. D. (2015). Aquatic metagenomes implicate Thaumarchaeota in global cobalamin production. *The ISME Journal*, *9*(2), 461-471. https://doi.org/10.1038/ismej.2014.142

Fiorella, K. J., Okronipa, H., Baker, K., & Heilpern, S. (2021). Contemporary aquaculture: implications for human nutrition. *Current Opinion in Biotechnology*, *70*, 83-90. https://doi.org/https://doi.org/10.1016/j.copbio.2020.11.014

Frankic, A., & Hershner, C. (2003). Sustainable aquaculture: developing the promise of aquaculture. *Aquaculture International*, *11*(6), 517-530. https://doi.org/10.1023/B:AQUI.0000013264.38692.91

Frette, L., Gejlsbjerg, B., & Westermann, P. (1997). Aerobic denitrifiers isolated from an alternating activated sludge system. *FEMS Microbiology Ecology*, *24*(4), 363-370. https://doi.org/10.1111/j.1574-6941.1997.tb00453.x

Graw, M. F., D'Angelo, G., Borchers, M., Thurber, A. R., Johnson, J. E., Zhang, C., Liu, H., & Colwell, F. S. (2018). Energy Gradients Structure Microbial Communities Across Sediment Horizons in Deep Marine Sediments of the South China Sea [Original Research]. *Frontiers in Microbiology*, *9*. https://doi.org/10.3389/fmicb.2018.00729

Grossman, A. (2016). Nutrient Acquisition: The Generation of Bioactive Vitamin B12 by Microalgae. *Current Biology*, *26*(8), R319-R321. https://doi.org/https://doi.org/10.1016/j.cub.2016.02.047

Hansell, D., Carlson, C. A., Repeta, D. J., & Schlitzer, R. (2009). DISSOLVED ORGANIC MATTER IN THE OCEAN: A CONTROVERSY STIMULATES NEW INSIGHTS. *Oceanography*, *22*(4), 202-211. https://www.jstor.org/stable/24861036

Harris, P., & Macmillan-Lawler, M. (2016). Global Overview of Continental Shelf Geomorphology Based on the SRTM30_ PLUS 30-Arc Second Database. In (Vol. 13, pp. 169-190). https://doi.org/10.1007/978-3-319-25121-9_7

Hayrapetyan, H., Tran, T., Tellez-Corrales, E., & Madiraju, C. (2023). Enzyme-Linked Immunosorbent Assay: Types and Applications. In R. S. Matson (Ed.), *ELISA: Methods and Protocols* (pp. 1-17). Springer US. https://doi.org/10.1007/978-1-0716-2903-1_1

He, H., Zhen, Y., Mi, T., Fu, L., & Yu, Z. (2018). Ammonia-Oxidizing Archaea and Bacteria Differentially Contribute to Ammonia Oxidation in Sediments from Adjacent Waters of Rushan Bay, China [Original Research]. *Frontiers in Microbiology*, *9*. https://doi.org/10.3389/fmicb.2018.00116

Heal, K. R., Qin, W., Ribalet, F., Bertagnolli, A. D., Coyote-Maestas, W., Hmelo, L. R., Moffett, J. W., Devol, A. H., Armbrust, E. V., Stahl, D. A., & Ingalls, A. E. (2017). Two distinct pools of B₁₂ analogs reveal community interdependencies in the ocean. *Proceedings of the National Academy of Sciences*, *114*(2), 364-369. https://doi.org/doi:10.1073/pnas.1608462114

Helliwell, Katherine E., Lawrence, Andrew D., Holzer, A., Kudahl, Ulrich J., Sasso, S., Kräutler, B., Scanlan, David J., Warren, Martin J., & Smith, Alison G. (2016). Cyanobacteria and Eukaryotic Algae Use Different Chemical Variants of Vitamin B12. *Current Biology*, *26*(8), 999-1008. https://doi.org/https://doi.org/10.1016/j.cub.2016.02.041

Hewitt, W. (1977a). CHAPTER 1 - INTRODUCTION. In W. Hewitt (Ed.), *Microbiological Assay* (pp. 1-16). Academic Press. https://doi.org/https://doi.org/10.1016/B978-0-12-346450-7.50005-9

Hewitt, W. (1977b). CHAPTER 2 - THE AGAR DIFFUSION ASSAY. In W. Hewitt (Ed.), *Microbiological Assay* (pp. 17-69). Academic Press. https://doi.org/https://doi.org/10.1016/B978-0-12-346450-7.50006-0

Inc., I. (2017). *An introduction to Next-Generation Sequencing Technology* https://www.illumina.com/content/dam/illumina-marketing/documents/products/illumina_sequencing_introduction.pdf

Jia, J., Gao, Y., Lu, Y., Shi, K., Li, Z., & Wang, S. (2020). Trace metal effects on gross primary productivity and its associative environmental risk assessment in a subtropical lake, China. *Environmental Pollution*, *259*, 113848. https://doi.org/https://doi.org/10.1016/j.envpol.2019.113848

Keeley, N., Valdemarsen, T., Woodcock, S., Holmer, M., Husa, V., & Bannister, R. (2019). Resilience of dynamic coastal benthic ecosystems in response to large-scale finfish farming. *Aquaculture Environment Interactions*, *11*, 161-179. https://www.int-res.com/abstracts/aei/v11/p161-179/

Kers, J. G., & Saccenti, E. (2021). The Power of Microbiome Studies: Some Considerations on Which Alpha and Beta Metrics to Use and How to Report Results. *Front Microbiol*, *12*, 796025. https://doi.org/10.3389/fmicb.2021.796025

Kralik, P., & Ricchi, M. (2017). A Basic Guide to Real Time PCR in Microbial Diagnostics: Definitions, Parameters, and Everything [Review]. *Frontiers in Microbiology*, *8*. https://doi.org/10.3389/fmicb.2017.00108

Kristensen, E. (2000). Organic matter diagenesis at the oxic/anoxic interface in coastal marine sediments, with emphasis on the role of burrowing animals. *Hydrobiologia*, *426*, 1-24. https://doi.org/10.1023/A:1003980226194

Kumar, P. S. (2021). *Chapter one - Introduction to marine biology*. Elsevier. https://doi.org/https://doi.org/10.1016/C2019-0-04371-3

Kumar, P. S. (2021). Chapter one - Introduction to marine biology. In P. S. Kumar (Ed.), *Modern Treatment Strategies for Marine Pollution* (pp. 1-10). Elsevier. https://doi.org/https://doi.org/10.1016/B978-0-12-822279-9.00008-7

Kumudha, A., Kumar, S. S., Thakur, M. S., Ravishankar, G. A., & Sarada, R. (2010). Purification, identification, and characterization of methylcobalamin from Spirulina platensis. *J Agric Food Chem*, *58*(18), 9925-9930. https://doi.org/10.1021/jf102159j

Laird, L. M. (2001). Mariculture Overview. In J. H. Steele (Ed.), *Encyclopedia of Ocean Sciences* (pp. 1572-1577). Academic Press. https://doi.org/https://doi.org/10.1006/rwos.2001.0474

Latta, T. N., Mandapat, A. L., & Myers, J. P. (2015). Anaerobic Spondylodiscitis due to Fusobacterium Species: A Case Report Review of the Literature. *Case Rep Infect Dis*, *2015*, 759539. https://doi.org/10.1155/2015/759539

Law, K. P., He, W., Tao, J., & Zhang, C. (2021). Characterization of the Exometabolome of Nitrosopumilus maritimus SCM1 by Liquid Chromatography–Ion Mobility Mass Spectrometry [Original Research]. *Frontiers in Microbiology*, *12*. https://doi.org/10.3389/fmicb.2021.658781

Lazzari, R., & Baldisserotto, B. (2008). Nitrogen and phosphorus waste in fish farming. *Boletim do Instituto de Pesca*, *34*, 591-600.

Lee, P. Y., Costumbrado, J., Hsu, C. Y., & Kim, Y. H. (2012). Agarose gel electrophoresis for the separation of DNA fragments. *J Vis Exp*(62). https://doi.org/10.3791/3923

Lenstra, J. A. (1995). The applications of the polymerase chain reaction in the life sciences. *Cell Mol Biol (Noisy-le-grand)*, *41*(5), 603-614.

Lønborg, C., Carreira, C., Jickells, T., & Salgado, X. À. À. (2020). Impacts of Global Change on Ocean Dissolved Organic Carbon (DOC) Cycling. *7*. https://www.frontiersin.org/articles/10.3389/fmars.2020.00466/full

Ma, A. T., Tyrell, B., & Beld, J. (2020). Specificity of cobamide remodeling, uptake and utilization in Vibrio cholerae. *Molecular Microbiology*, *113*.

Magra, I. (2019). Millions of Salmon in Norway Killed by Algae Bloom. *The New York Times*. https://www.nytimes.com/2019/05/23/world/europe/salmon-norway-algae-bloom.html

McElroy, W. D., & Swanson, C. P. (1953). Trace Elements. *Scientific American*, *188*(1), 22-25. http://www.jstor.org/stable/24944097

McMurdie, P. J., & Holmes, S. (2013). phyloseq: An R Package for Reproducible Interactive Analysis and Graphics of Microbiome Census Data. https://journals.plos.org/plosone/article?id=10.1371/journal.pone.0061217

Mestan, K., Ilkhanoff, L., Mouli, S., & Lin, S. (2011). Genomic sequencing in clinical trials. *Journal of translational medicine*, *9*, 222. https://doi.org/10.1186/1479-5876-9-222

Morel, F., Milligan, A., & Saito, M. (2003). Marine Bioinorganic Chemistry: The Role of Trace Metals in the Oceanic Cycles of Major Nutrients. *Treatise on Geochemistry*, *6*, 113-143. https://doi.org/10.1016/B0-08-043751-6/06108-9

Morel, F. M. M. (2000). Use of Trace Metals in: Marine Bioremediation: A Need for Fundamental Knowledge. In

Opportunities for Environmental Applications of Marine Biotechnology: Proceedings of the October 5-6, 1999, Workshop (pp. 96-101). The National Academies Press. https://doi.org/doi:10.17226/9988

N. Jiao, C. Robinson, F. Azam, H. Thomas, F. Baltar, H. Dang, N. J. Hardman-Mountford, M. Johnson, D. L. K., B. P. Koch, L. L., C. Li, J. L., T. Luo, Y.-W. Luo, A. Mitra, A. Romanou, K. Tang, X. W., C. Zhang, & Zhang, R. (2014). Mechanisms of microbial carbon sequestration in the ocean – future research directions. *Biogeosciences*, *11*(19), 5285-5306. https://doi.org/https://doi.org/10.5194/bg-11-5285-2014

Naylor, R. L., Hardy, R. W., Buschmann, A. H., Bush, S. R., Cao, L., Klinger, D. H., Little, D. C., Lubchenco, J., Shumway, S. E., & Troell, M. (2021). A 20-year retrospective review of global aquaculture. *Nature*, *591*(7851), 551-563. https://doi.org/10.1038/s41586-021-03308-6

Nishijima, T., & Hata, Y. (1986). Distribution of Vitamin B₁₂, Thiamine, and Biotin in the Water of Harima-Nada Sea. *Nippon Suisan Gakkaishi*, *52*(9), 1533-1545. https://doi.org/10.2331/suisan.52.1533

Nunnally, C. C. (2019). Benthic–Pelagic Coupling: Linkages Between Benthic Ecology and Biogeochemistry and Pelagic Ecosystems and Process. In *Encyclopedia of Ocean Sciences (Third Edition)* (Vol. 2). Elsevier Ltd. https://doi.org/https://doi.org/10.1016/B978-0-12-409548-9.11087-5

Olaussen, J. O. (2018). Environmental problems and regulation in the aquaculture industry. Insights from Norway. *Marine Policy*, *98*, 158-163. https://doi.org/https://doi.org/10.1016/j.marpol.2018.08.005

Oohora, K., & Hayashi, T. (2016). Chapter Nineteen - Reconstitution of Heme Enzymes with Artificial Metalloporphyrinoids. In V. L. Pecoraro (Ed.), *Methods in Enzymology* (Vol. 580, pp. 439-454). Academic Press. https://doi.org/https://doi.org/10.1016/bs.mie.2016.05.049

Orcutt, B., Sylvan, J., Knab, N., & Edwards, K. (2011). Microbial Ecology of the Dark Ocean above, at, and below the Seafloor. *Microbiology and Molecular Biology Reviews*, 361–422. https://doi.org/10.1128/MMBR.00039-10

Orsi, W. D. (2018). Ecology and evolution of seafloor and subseafloor microbial communities. *Nat Rev Microbiol*, *16*(11), 671-683. https://doi.org/10.1038/s41579-018-0046-8

Osman, D., Cooke, A., Young, T. R., Deery, E., Robinson, N. J., & Warren, M. J. (2021). The requirement for cobalt in vitamin B12: A paradigm for protein metalation. *Biochimica et Biophysica Acta (BBA) - Molecular Cell Research*, *1868*(1), 118896. https://doi.org/https://doi.org/10.1016/j.bbamcr.2020.118896

Passow, U. (2002). Transparent exopolymer particles (TEP) in aquatic environments. *Progress in Oceanography*, *55*(3), 287-333. https://doi.org/https://doi.org/10.1016/S0079-6611(02)00138-6

Petrosino, J. F., Highlander, S., Luna, R. A., Gibbs, R. A., & Versalovic, J. (2009). Metagenomic Pyrosequencing and Microbial Identification. *Clinical Chemistry*, *55*(5), 856-866. https://doi.org/10.1373/clinchem.2008.107565

Pettersen, R., Ormaasen, I., Angell, I. L., Keeley, N. B., Lindseth, A., Snipen, L., & Rudi, K. (2022). Bimodal distribution of seafloor microbiota diversity and function are associated with marine aquaculture. *Marine Genomics*, *66*, 100991. https://doi.org/https://doi.org/10.1016/j.margen.2022.100991

Pikelj, K., Uroš, A., Kolda, A., Gavrilović, A., & Kapetanović, D. (2022). Sediment Characteristics—A Key Factor for Fish Farm Site Selection: Examples from Croatia. *Minerals*, *12*(6), 696. https://www.mdpi.com/2075-163X/12/6/696

Pinto, O., Silva, T., Vizzotto, C., Santana, R., Lopes, F., Silva, B., Thompson, F., & Krüger, R. (2020). Genome-resolved metagenomics analysis provides insights into the ecological role of Thaumarchaeota in the Amazon River and its plume. *BMC Microbiology*, *20*. https://doi.org/10.1186/s12866-020-1698-x

Piontek, J., Galgani, L., Nöthig, E.-M., Peeken, I., & Engel, A. (2021). Organic matter composition and heterotrophic bacterial activity at declining summer sea ice in the central Arctic Ocean. *Limnology and Oceanography*, *66*(S1), S343-S362. https://doi.org/https://doi.org/10.1002/lno.11639

Piwowarek, K., Lipińska, E., Hać-Szymańczuk, E., Kieliszek, M., & Ścibisz, I. (2018). Propionibacterium spp.—source of propionic acid, vitamin B12, and other metabolites

important for the industry. *Applied Microbiology and Biotechnology*, *102*(2), 515-538. https://doi.org/10.1007/s00253-017-8616-7

Polidoro, B. A., Carpenter, K. E., Collins, L., Duke, N. C., Ellison, A. M., Ellison, J. C., Farnsworth, E. J., Fernando, E. S., Kathiresan, K., Koedam, N. E., Livingstone, S. R., Miyagi, T., Moore, G. E., Ngoc Nam, V., Ong, J. E., Primavera, J. H., Salmo, S. G., III, Sanciangco, J. C., Sukardjo, S., . . . Yong, J. W. H. (2010). The Loss of Species: Mangrove Extinction Risk and Geographic Areas of Global Concern. *PLOS ONE*, *5*(4), e10095. https://doi.org/10.1371/journal.pone.0010095

Polimene, L., Sailley, S., Clark, D., Mitra, A., & Allen, J. (2017). Biological or microbial carbon pump? The role of phytoplankton stoichiometry in ocean carbon sequestration. *Journal of Plankton Research*, *39*(2), 180-186. https://doi.org/https://doi.org/10.1093/plankt/fbw091 (22.12.16)

Rabus, R., Hansen, T. A., & Widdel, F. (2013). Dissimilatory Sulfate- and Sulfur-Reducing Prokaryotes. In E. Rosenberg, E. F. DeLong, S. Lory, E. Stackebrandt, & F. Thompson (Eds.), *The Prokaryotes: Prokaryotic Physiology and Biochemistry* (pp. 309-404). Springer Berlin Heidelberg. https://doi.org/10.1007/978-3-642-30141-4_70

Raina, V., Nayak, T., Ray, L., Kumari, K., & Suar, M. (2019). Chapter 9 - A Polyphasic Taxonomic Approach for Designation and Description of Novel Microbial Species. In S. Das & H. R. Dash (Eds.), *Microbial Diversity in the Genomic Era* (pp. 137-152). Academic Press. https://doi.org/https://doi.org/10.1016/B978-0-12-814849-5.00009-5

Rapin, A., Pattaroni, C., Marsland, B. J., & Harris, N. L. (2017). Microbiota Analysis Using an Illumina MiSeq Platform to Sequence 16S rRNA Genes. *Current Protocols in Mouse Biology*, *7*(2), 100-129. https://doi.org/https://doi.org/10.1002/cpmo.29

Raux, E., Schubert, H. L., & Warren*, M. J. (2000). Biosynthesis of cobalamin (vitamin B12): a bacterial conundrum. *Cellular and Molecular Life Sciences CMLS*, *57*(13), 1880-1893. https://doi.org/10.1007/PL00000670

Reen, D. J. (1994). Enzyme-linked immunosorbent assay (ELISA). *Methods Mol Biol*, *32*, 461-466. https://doi.org/10.1385/0-89603-268-x:461

Rhoads, A., & Au, K. F. (2015). PacBio Sequencing and Its Applications. *Genomics, Proteomics & Bioinformatics*, *13*(5), 278-289. https://doi.org/https://doi.org/10.1016/j.gpb.2015.08.002

Rognes, T., Flouri, T., Nichols, B., Quince, C., & Mahé, F. (2016). VSEARCH: a versatile open source tool for metagenomics. *PeerJ*. https://doi.org/10.7717/peerj.2584

Saba, G. K., Steinberg, D. K., & Bronk, D. (2011). The relative importance of sloppy feeding, excretion, and fecal pellet leaching in the release of dissolved carbon and nitrogen by Acartia tonsa copepods. *Journal of Experimental Marine Biology and Ecology*, *404*(1-2), 47-56. https://doi.org/https://doi.org/10.1016/j.jembe.2011.04.013

Sakamoto, S., Putalun, W., Vimolmangkang, S., Phoolcharoen, W., Shoyama, Y., Tanaka, H., & Morimoto, S. (2018). Enzyme-linked immunosorbent assay for the quantitative/qualitative analysis of plant secondary metabolites. *J Nat Med*, *72*(1), 32-42. https://doi.org/10.1007/s11418-017-1144-z

Santos, A., van Aerle, R., Barrientos, L., & Martinez-Urtaza, J. (2020). Computational methods for 16S metabarcoding studies using Nanopore sequencing data. *Computational and Structural Biotechnology Journal*, *18*. https://doi.org/10.1016/j.csbj.2020.01.005

Schoffman, H., Lis, H., Shaked, Y., & Keren, N. (2016). Iron–Nutrient Interactions within Phytoplankton [Review]. *Frontiers in Plant Science*, *7*. https://doi.org/10.3389/fpls.2016.01223

Shendure, J., & Ji, H. (2008). Next-generation DNA sequencing. *Nature Biotechnology*, *26*(10), 1135-1145. https://doi.org/10.1038/nbt1486

Sigman, D., & Hain, M. (2012). The Biological Productivity of the Ocean. *Nature Education*, *3*, 1-16.
Simon, J., & Kroneck, P. M. H. (2013). Chapter Two - Microbial Sulfite Respiration. In R. K. Poole (Ed.), *Advances in Microbial Physiology* (Vol. 62, pp. 45-117). Academic Press. https://doi.org/https://doi.org/10.1016/B978-0-12-410515-7.00002-0
Skirrow, M. B. (2003). CAMPYLOBACTER | Properties and Occurrence. In B. Caballero (Ed.), *Encyclopedia of Food Sciences and Nutrition (Second Edition)* (pp. 779-786). Academic Press. https://doi.org/https://doi.org/10.1016/B0-12-227055-X/00151-6
Snelgrove, P., T, B., Hutchings, P., Alongi, D., J, G., Hummel, H., King, G., Koike, I., Lambshead, P. J., Ramsing, N., & Solís-Weiss, V. (1997). The importance of marine sediment biodiversity in ecosystem processes. *Ambio*, *26*, 578-583.
Spohn, S. N., & Young, V. B. (2018). Chapter 32 - Gastrointestinal Microbial Ecology With Perspectives on Health and Disease. In H. M. Said (Ed.), *Physiology of the Gastrointestinal Tract (Sixth Edition)* (pp. 737-753). Academic Press. https://doi.org/https://doi.org/10.1016/B978-0-12-809954-4.00032-3
Stieglmeier, M., Alves, R. J. E., & Schleper, C. (2014). The Phylum Thaumarchaeota. In E. Rosenberg, E. F. DeLong, S. Lory, E. Stackebrandt, & F. Thompson (Eds.), *The Prokaryotes: Other Major Lineages of Bacteria and The Archaea* (pp. 347-362). Springer Berlin Heidelberg. https://doi.org/10.1007/978-3-642-38954-2_338
Taksdal, G., & Hågvar, S. (2001). *Økologi og miljøvern*. Landbruksforlaget.
Taranger, G. L., Karlsen, Ø., Bannister, R. J., Glover, K. A., Husa, V., Karlsbakk, E., Kvamme, B. O., Boxaspen, K. K., Bjørn, P. A., Finstad, B., Madhun, A. S., Morton, H. C., & Svåsand, T. (2014). Risk assessment of the environmental impact of Norwegian Atlantic salmon farming. *ICES Journal of Marine Science*, *72*(3), 997-1021. https://doi.org/10.1093/icesjms/fsu132
Teira, E., Reinthaler, T., Pernthaler, A., Pernthaler, J., & Herndl, G. J. (2004). Combining catalyzed reporter deposition-fluorescence in situ hybridization and microautoradiography to detect substrate utilization by bacteria and Archaea in the deep ocean. *Appl Environ Microbiol*, *70*(7), 4411-4414. https://doi.org/10.1128/aem.70.7.4411-4414.2004
Trombetta, T., Vidussi, F., Roques, C., Scotti, M., & Mostajir, B. (2020). Marine Microbial Food Web Networks During Phytoplankton Bloom and Non-bloom Periods: Warming Favors Smaller Organism Interactions and Intensifies Trophic Cascade. *Aquatic Microbiology*, *11*. https://doi.org/https://doi.org/10.3389/fmicb.2020.502336
Tsiami, A., & Obersby, D. (2017). 41 - B Vitamins Intake and Plasma Homocysteine in Vegetarians. In F. Mariotti (Ed.), *Vegetarian and Plant-Based Diets in Health and Disease Prevention* (pp. 747-767). Academic Press. https://doi.org/https://doi.org/10.1016/B978-0-12-803968-7.00041-1
Valdemarsen, T., Bannister, R. J., Hansen, P. K., Holmer, M., & Ervik, A. (2012). Biogeochemical malfunctioning in sediments beneath a deep-water fish farm. *Environmental Pollution*, *170*, 15-25. https://doi.org/https://doi.org/10.1016/j.envpol.2012.06.007
Ward, B. B. (2003). Significance of anaerobic ammonium oxidation in the ocean. *Trends in Microbiology*, *11*(9), 408-410. https://doi.org/https://doi.org/10.1016/S0966-842X(03)00181-1
Wehrmann, L. M., & Ferdelman, T. G. (2014). Chapter 2.7 - Biogeochemical Consequences of the Sedimentary Subseafloor Biosphere. In R. Stein, D. K. Blackman, F. Inagaki, & H.-C. Larsen (Eds.), *Developments in Marine Geology* (Vol. 7, pp. 217-252). Elsevier. https://doi.org/https://doi.org/10.1016/B978-0-444-62617-2.00009-8

Wienhausen, G., Dlugosch, L., Jarling, R., Wilkes, H., Giebel, H.-A., & Simon, M. (2022). Availability of vitamin B12 and its lower ligand intermediate α-ribazole impact prokaryotic and protist communities in oceanic systems. *The ISME Journal*, *16*(8), 2002-2014. https://doi.org/10.1038/s41396-022-01250-7

Williams, M. J. (1999). The role of fisheries and aquaculture in the future supply of animal protein In *Sustainable Aquaculture* (pp. 5-15). A.A. Balkema.

Willis, A. D. (2019). Rarefaction, Alpha Diversity, and Statistics [Perspective]. *Frontiers in Microbiology*, *10*. https://doi.org/10.3389/fmicb.2019.02407

Xu, W., Shin, P. K. S., & Sun, J. (2022). Organic Enrichment Induces Shifts in the Trophic Position of Infauna in a Subtropical Benthic Food Web, Hong Kong [Brief Research Report]. *Frontiers in Marine Science*, *9*. https://doi.org/10.3389/fmars.2022.937477

Yu, Y., Lee, C., Kim, J., & Hwang, S. (2005). Group-specific primer and probe sets to detect methanogenic communities using quantitative real-time polymerase chain reaction. *Biotechnology and Bioengineering*, *89*(6), 670-679. https://doi.org/https://doi.org/10.1002/bit.20347

Supplementary materials

S.1 Index primers

Table S.1 Index primer sequences that were used for indexing samples for 16S rRNA Illumina Miseq sequencing. The table shows 8 forward and 23 reverse primers and their corresponding sequences utilized during Index PCR (Yu et al., 2005).

Primers	Sequence (5'-3')
F1	aatgatacggcgaccaccgagatctacactctttccctacacgacgctcttccgatctagtcaaCCTACGGGRBGCASCAG
F2	aatgatacggcgaccaccgagatctacactctttccctacacgacgctcttccgatctagttccCCTACGGGRBGCASCAG
F3	aatgatacggcgaccaccgagatctacactctttccctacacgacgctcttccgatctatgtcaCCTACGGGRBGCASCAG
F4	aatgatacggcgaccaccgagatctacactctttccctacacgacgctcttccgatctccgtccCCTACGGGRBGCASCAG
F5	aatgatacggcgaccaccgagatctacactctttccctacacgacgctcttccgatctgtagagCCTACGGGRBGCASCAG
F6	aatgatacggcgaccaccgagatctacactctttccctacacgacgctcttccgatctgtccgcCCTACGGGRBGCASCAG
F7	aatgatacggcgaccaccgagatctacactctttccctacacgacgctcttccgatctgtgaaaCCTACGGGRBGCASCAG
F8	aatgatacggcgaccaccgagatctacactctttccctacacgacgctcttccgatctgtggccCCTACGGGRBGCASCAG
R1	caagcagaagacggcatacgagatCGTGATgtgactggagttcagacgtgtgctcttccgatctGGACTACYVGGGTATCTAAT
R2	caagcagaagacggcatacgagatACATCGgtgactggagttcagacgtgtgctcttccgatctGGACTACYVGGGTATCTAAT
R3	caagcagaagacggcatacgagatGCCTAAgtgactggagttcagacgtgtgctcttccgatctGGACTACYVGGGTATCTAAT
R4	caagcagaagacggcatacgagatTGGTCAgtgactggagttcagacgtgtgctcttccgatctGGACTACYVGGGTATCTAAT
R5	caagcagaagacggcatacgagatCACTCTgtgactggagttcagacgtgtgctcttccgatctGGACTACYVGGGTATCTAAT
R6	caagcagaagacggcatacgagatATTGGCgtgactggagttcagacgtgtgctcttccgatctGGACTACYVGGGTATCTAAT
R7	caagcagaagacggcatacgagatGATCTGgtgactggagttcagacgtgtgctcttccgatctGGACTACYVGGGTATCTAAT
R8	caagcagaagacggcatacgagatTCAAGTgtgactggagttcagacgtgtgctcttccgatctGGACTACYVGGGTATCTAAT
R9	caagcagaagacggcatacgagatCTGATCgtgactggagttcagacgtgtgctcttccgatctGGACTACYVGGGTATCTAAT
R20	caagcagaagacggcatacgagatAAGCTAgtgactggagttcagacgtgtgctcttccgatctGGACTACYVGGGTATCTAAT
R21	caagcagaagacggcatacgagatGTAGCCgtgactggagttcagacgtgtgctcttccgatctGGACTACYVGGGTATCTAAT
R22	caagcagaagacggcatacgagatTACAAGgtgactggagttcagacgtgtgctcttccgatctGGACTACYVGGGTATCTAAT
R23	caagcagaagacggcatacgagatTTGACTgtgactggagttcagacgtgtgctcttccgatctGGACTACYVGGGTATCTAAT

F: forward, R: reverse, Target gene/region: 16S rRNA (V3-V4)

S.2 Trace mineral components (100 mL)

- 0.8 ml conc. HCl (~12.5 M)
- 3.0 mg H_3BO_3
- 10.0 mg $MnCl_2 \cdot 4H_2O$
- 19.0 mg $CoCl_2 \cdot 6H_2O$
- 2.4 mg $NiCl_2 \cdot 6H_2O$
- 0.2 mg $CuCl_2 \cdot 2H_2O$
- 14.4 mg $ZnSO_4 \cdot 7H_2O$
- 3.6 mg $Na_2MoO_4 \cdot 2H_2O$
- 99.2 ml deionized H_2O (MilliQ)

S.3 Agar plates

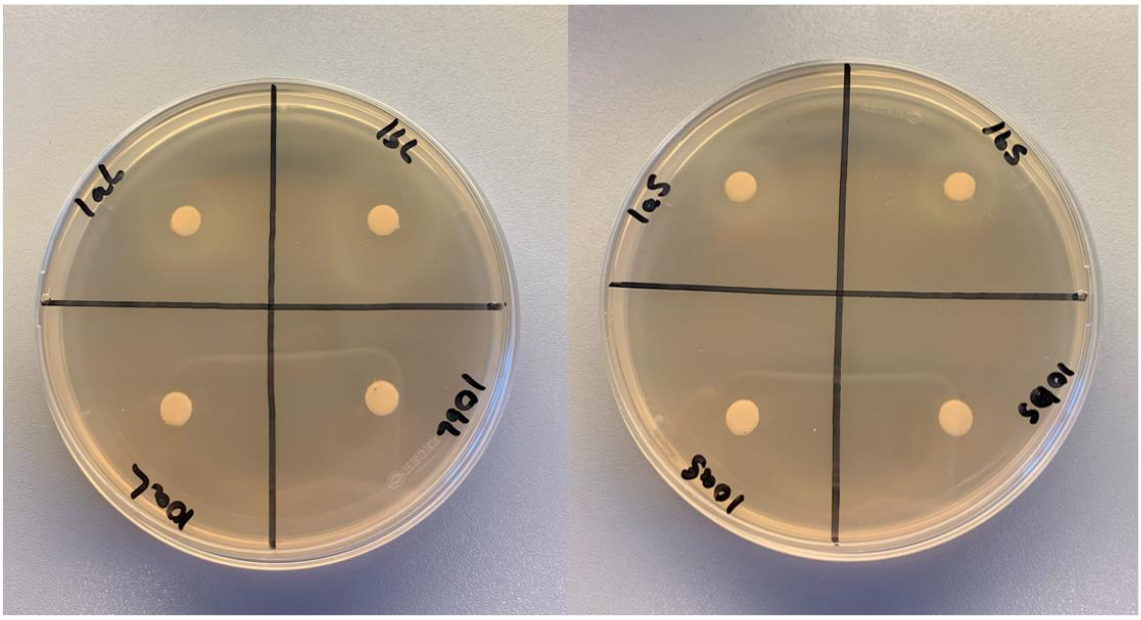

Supplementary material S.3.1: Comparison of growth zones when mechanical lysis was omitted (left photo) and when it was not (right photo) and when autoclaving was performed (a) and when it was not (b). 1 = 1000 ng/L and 10: 0 ng/L of spiked cobalamin. a: autoclaved and b: not autoclaved. L: mechanical lysis was omitted and S: mechanical lysis was performed. Cobalamin standards are missing.

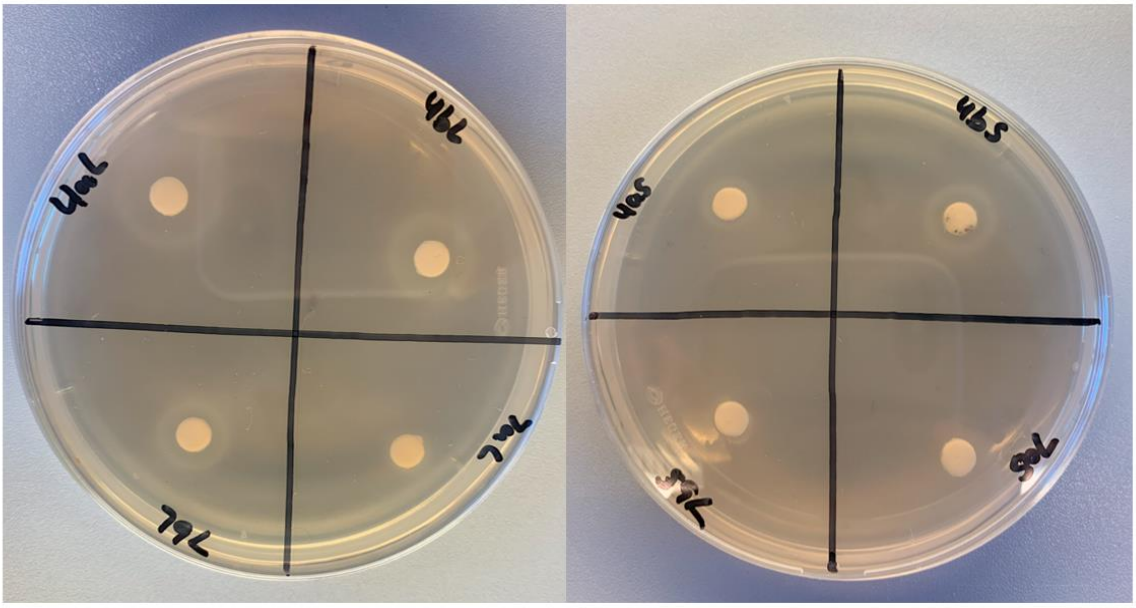

Supplementary material S.3.2: Comparison of growth zones when mechanical lysis was omitted (left photo) and when it was not (right photo) and when autoclaving was performed (a) and when it was not (b). 4 = 100 ng/L and 17: 10 ng/L of spiked cobalamin. a: autoclaved and b: not autoclaved. L: mechanical lysis was omitted and S: mechanical lysis was performed. Cobalamin standards are missing.

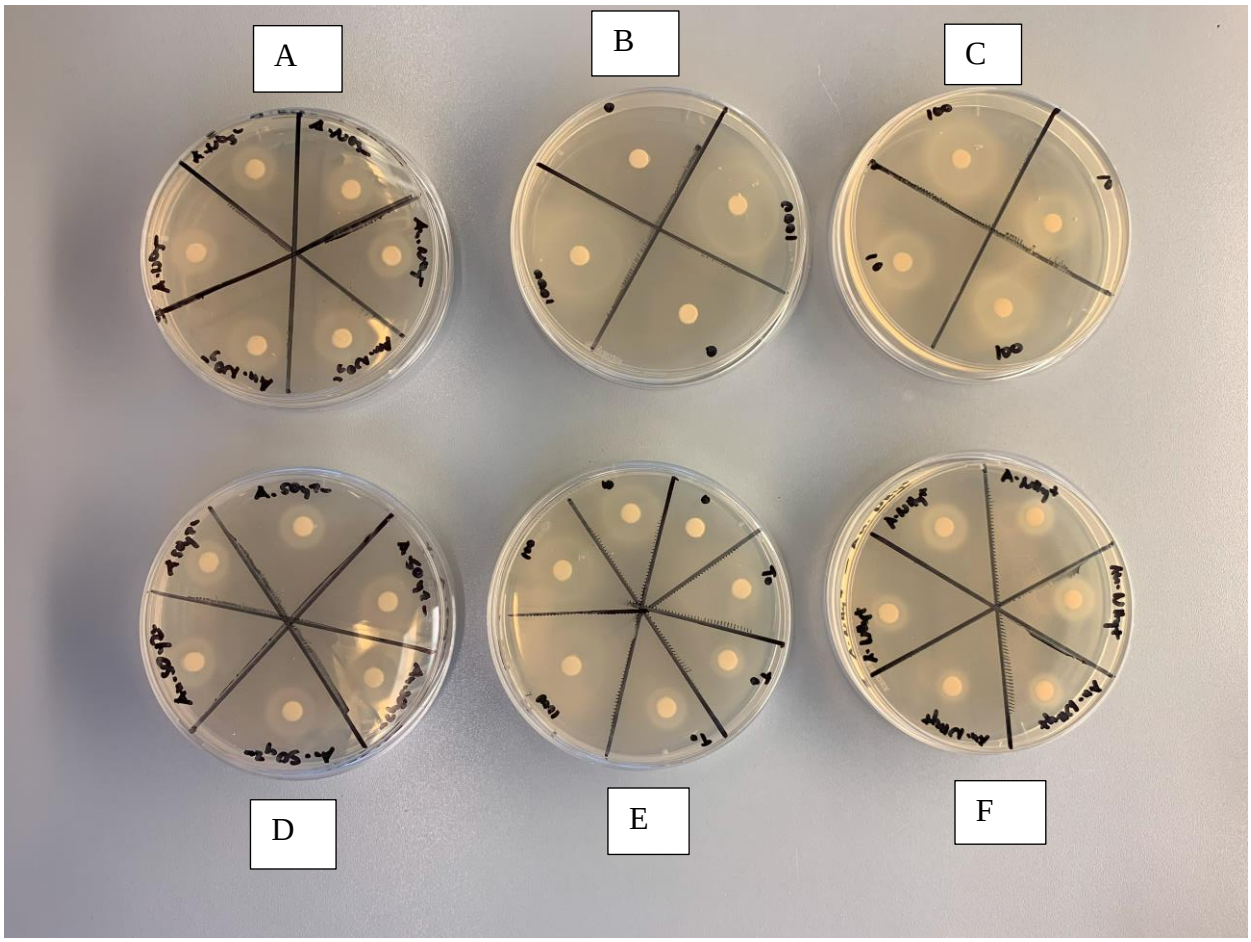

Supplementary material S.3.3 Illustration of growth zones from the samples from T8 after performing the optimized protocol. A) Nitrate-reducing media plate. B) 1000 and 0 ng/mL plate. C) 100 and 10 ng/mL plate. D) Sulfate-reducing plate. E) Standard: 1000, 100, 10, 0 ng/mL and T0 plate. F) Ammonium-oxidizing plate. A: oxic, An: anoxic. NO_3^-: nitrate-reducing, SO_4^{2-}: sulfate-reducing, NH_4^+: ammonium-oxidizing. Cobalamin standards are present.

Norges miljø- og biovitenskapelige universitet
Noregs miljø- og biovitskapelege universitet
Norwegian University of Life Sciences

Postboks 5003
NO-1432 Ås
Norway